2) วิเคราะห์แบบ 3D เพื่อศึกษาการเกิด โครงสร้างเกรนก้อนกลมในระยะเริ่มต้น

เอกสารอ้างอิง

- [1] Campbell J. Castings. Butterworth-Heinemann, Oxford, 1991.
- [2] The North American Die Casting Association. http://www.nadca.org.
- [3] Vinarcik E. High Integrity Die Casting Processes. Wiley-Interscience, 2002.
- [4] UBE Machinery, Inc. http://www.ubemachinery.com/diecasting.html.
- [5] Martinez R. "Formation and Processing of Rheocast Microstructures." Ph.D. Thesis, Massachusetts Institute of Technology, Cambridge, MA, USA, 2004.
- [6] Vforge, Inc. http://www.vforge.com/
- [7] deFigueredo A, Ed. *Science and Technology of Semi-Solid Metal Processing*, The North American Die Casting Association, 2001.
- [8] Jorstad J, *et al.*, Proceedings of the 8th International Conference on Semi-Solid Processing of Alloys and Composites, Limassol, Cyprus, September 21–23, 2004.
- [9] Yurko J., *et al.* Proceedings of the 8th International Conference on Semi-Solid Processing of Alloys and Composites, Limassol, Cyprus, September 21–23, 2004.
- [10] Wannasin J, et al., ScriptaMaterialia. 55 (2006) 115-118.
- [11] Iqbal N, et al., Acta Mater. 53 (2005) 2875-2880.
- [12] Nafisi N and Ghomashchi R, Mater. Sci. Eng. 437A (2006) 388-395.
- [13] Wu S, et al., Scripta Mater. 58 (2008) 556-559.
- [14] Jian X, et al., Mater. Letters. 59 (2005) 190-193.
- [15] Li T, et al., Acta Mater. 54 (2006) 4815-4824.
- [16] Flemings MC. Solidification Processing. McGraw-Hill, 1974.
- [17] Yang Z, et al., Metall. Mater. Trans. A. 36A (2005) 2785-2792.
- [18] Das A, et al., ActaMaterialia. 50 (2002) 4571-4585.
- [19] Jackson KA, et al., Trans. Metall. Soc. AIME. 236 (1966) 149-158.
- [20] Hellawell A, et al., JOM (1997) 18-20.
- [21] Ji S. J. Mater. Sci. 38 (2003) 1559-1564.
- [22] Ruvalcaba D, et al., Acta Mater. 55 (2007) 4287-4292.

สิ่งที่ได้รับ (Output) จากโครงการ

1. วารสารระดับนานาชาติที่มี Impact Factor (International Journal with Impact factor)

ผลการวิจัยของโครงการนี้ได้นำไปตีพิมพ์โดยตรงและนำไปประยุกต์ในโครงการวิจัยอื่นและทำให้ เกิดผลงานตีพิมพ์จำนวน 4 ชิ้น โดยที่มีผลงานอีก 2 ชิ้นอยู่ในระหว่างการเตรียมส่งตีพิมพ์ รายละเอียดผลงาน ที่ตีพิมพ์แล้วมีดังนี้

- 1. **Wannasin J**, Janudom S, Rattanochaikul T, Canyook R, Burapa R, Chucheep T, Thanabumrungkul S. *Research and development of gas induced semi-solid process for industrial applications*. Transactions of Nonferrous Metals Society of China, 20 (2010), p. s1010-s1015.
- 2. Canyook R, Petsut S, Wisutmethangoon S, Flemings MC, Wannasin J. Evolution of microstructure in semi-solid slurries of rheocast aluminum alloy. Transactions of Nonferrous Metals Society of China, 20 (2010), p. 1649-1655.
- 3. JanudomS, Rattanochaikul T, Burapa R, Wisutmethangoon S, **Wannasin J**. Feasibility of semi-solid die casting of ADC12 aluminum alloy. Transactions of Nonferrous Metals Society of China, 20 (2010), p. 1756-1762.
- 4. Rattanochaikul T, Janudom S, Memongkol N, **Wannasin J**. *Development of aluminum rheo-extrusion process usingsemi-solid slurry at low solid fraction*. Transactions of Nonferrous Metals Society of China, 20 (2010), p. 1763-1768.

2. การนำผลงานวิจัยไปใช้ประโยชน์

งานวิจัยนี้ได้ผลิตนักศึกษาทั้งระดับปริญญาตรีปริญญาโท และปริญญาเอก หลายคนซึ่งได้ร่วมงาน วิจัยและเรียนรู้ในโครงการวิจัยนี้ ซึ่งประกอบไปด้วย

- นางสาวรังสินี แคนยุกต์
- นายสมใจ จันทร์อุคม
- นายเธียรศักดิ์ ชูชีพ
- นายธเนศ รัตโนชัยกุล
- นางสาวบัวแสง กาญจนดิษฐ์
- นางสาวมาณวิกา คงพ่วง

ภาคผนวก ก. วารสารวิชาการ ระดับนานาชาติ 4 ฉบับ



Available online at www.sciencedirect.com



Trans. Nonferrous Met. Soc. China 20(2010) s1010-s1015

Transactions of Nonferrous Metals Society of China

www.tnmsc.cn

Research and development of gas induced semi-solid process for industrial applications

J. WANNASIN¹, S. JANUDOM¹, T. RATTANOCHAIKUL¹, R. CANYOOK¹, R. BURAPA², T. CHUCHEEP¹, S. THANABUMRUNGKUL¹

- 1. Department of Mining and Materials Engineering, Faculty of Engineering, Prince of Songkla University, Hat Yai, Songkhla, 90112, Thailand;
- 2. Department of Industrial Engineering, Faculty of Engineering, Rajamangala University of Technology Srivijaya, Songkhla, 90000, Thailand

Received 13 May 2010; accepted 25 June 2010

Abstract: Several rheocasting processes are developed or applied worldwide in the metal forming industry. One of the new rheocasting processes is the gas induced semi-solid (GISS) process. The GISS process utilizes the principle of rapid heat extraction and vigorous local extraction using the injection of fine gas bubbles through a graphite diffuser. Several forming processes such as die casting, squeeze casting, gravity casting, and rheo-extrusion of the semi-solid slurries prepared by the GISS process have also been conducted. The GISS process is capable of processing various alloys including cast aluminum alloys, die casting aluminum alloys, wrought aluminum alloys, and zinc alloys. The GISS process is currently developed to be used commercially in the industry with the focus on forming semi-solid slurries containing low fractions solid (< 0.25) into parts. The research and development activities of the GISS process were discussed and the status of the industrial developments of this process was reported.

Key words: gas induced semi-solid; rheocasting; die casting; formation mechanism; industrial applications

1 Introduction

Semi-solid metal forming employing rheocasting approach has attracted interests in recent years[1-3]. The needs to produce high quality parts with lower costs are the driving force for this attention. Several techniques are applied in the worldwide industry including the NRC[4], SLC[5], SSR[6], rheo-die casting[7], rapid-S[8], and several more[9]. One of the newer techniques that are in the research and development stage is the gas induced semi-solid(GISS) process[10-13]. This process utilizes the principle of rapid heat extraction and vigorous local extraction using the injection of fine gas bubbles through a graphite diffuser. Semi-solid slurries with different solid fractions can be obtained simply by varying the diffuser immersion times.

The current focus of the GISS process is on forming semi-solid slurries containing low fractions solid (< 0.25) into parts. This allows prompt exploitation of the benefits of semi-solid metal in several forming processes since

little modifications to the current machines and processing steps are required[14]. Previous studies have shown that the GISS process can be applied conveniently and efficiently with a die casting machine, requiring only minimal modifications of the process[13]. In addition, the process has been shown to be able to produce slurries of various alloys, including those with the compositions close to the eutectic composition[12–13].

To demonstrate its commercial potential, it is important that the research and development activities of the GISS process shift from laboratory scale to industrial scale. This work aims to discuss the research and development activities of the GISS process that are carried out and to report the status of the industrial developments of this process.

2 GISS process

Current rheocasting processes use different techniques to produce metal slurries. Most of them, however, utilize the application of agitation to a molten

coupled with controlled cooling during solidification to achieve grain multiplication by dendrite fragmentation[14-16]. Examples of the processes include mechanical stirring[17], electromagnetic stirring[18], low-temperature casting[19-20], ultrasonic vibrations[21–22]. These techniques use different media or means to apply agitation to the melt such as solid impellers or cylindrical rods, electromagnetic force, from flow, convection fluid and respectively[11]. The GISS process, on the other hand, induces vigorous convection to the melt using fine gas bubbles as the medium. Various configurations may be used to introduce the fine gas bubbles to the melt, including gas injection through a nozzle or through porous media as presented schematically in Fig.1[23]. Currently, the configuration shown in Fig.1(c) is selected to use in the GISS machine due to its efficiency and simplicity. In the GISS process, the steps start by having a molten metal with a predetermined amount at a temperature about 10 to 20°C above the liquidus temperature. Then, the porous graphite diffuser is immersed, injecting fine inert gas bubbles into the melt for a predetermined time until the desired solid fraction is achieved. Consequently, the semi-solid slurry is formed and is ready for a further forming step. Fig.2 shows the processing steps schematically in the GISS process.

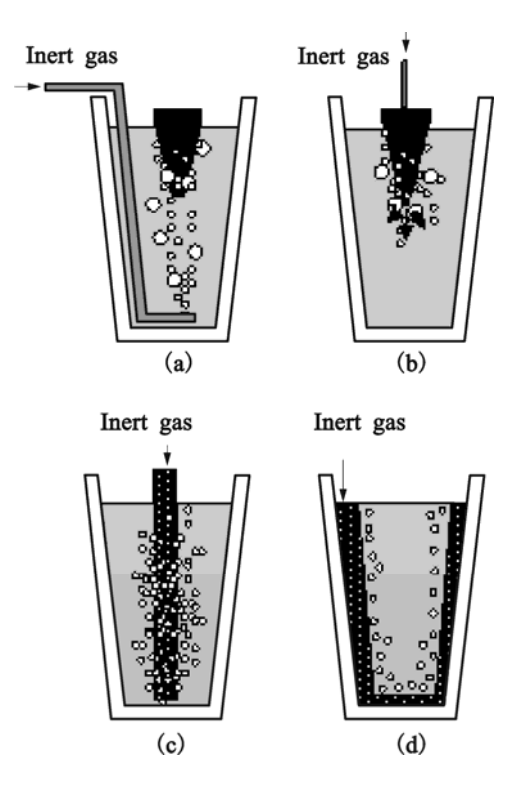


Fig.1 Examples of possible configurations for introducing fine gas bubbles to melt[23]

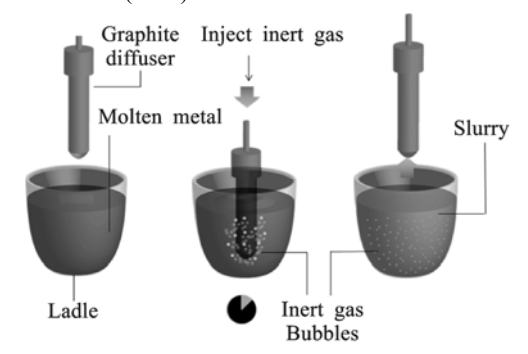


Fig.2 Schematic representation of steps in GISS process

3 Formation mechanism

The exact mechanism for semi-solid metal structure formation is still unclear. However, it is well accepted that the globular structure is obtained when numerous solid grains are present at the early stages of solidification[24]. Then, the high density of the solid grains grows non-dendritically, resulting in semi-solid metal structure[25].

The likely theory that can explain how a large number of solid particles are formed is grain multiplication by dendrite fragmentation[26]. It has been proposed that the convection produced during the solidification causes dendrite arms to be detached by melting off or breaking off. These detached arms then act as secondary nuclei particles. A schematic diagram of the dendrite multiplication theory is shown in Fig.3.

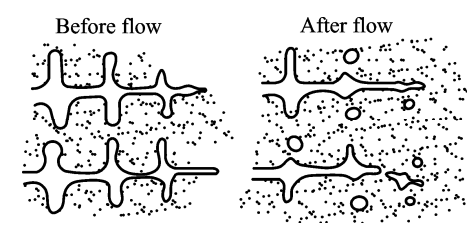


Fig.3 Schematic diagram of dendrite multiplication model[27]

In the GISS process, convection is effectively achieved by the flow of a large number of very fine gas bubbles out of the cold diffuser surfaces into the melt. This vigorous convection is believed to cause grain multiplication, resulting in a large number of fine disintegrated solid particles.

Using a rapid quenching mold, a study has shown the evolution of grain particles of A380 alloy at various time during the GISS process (Fig.4)[28]. The micrographs show that the microstructure consists of a mixture of globular, rosette, and dendrite particles at the early stages of the rheocasting process. These globular and the rosette particles are believed to be the disintegrated particles resulting from the dendrite fragmentation due to the remelting mechanism. This mechanism explains that

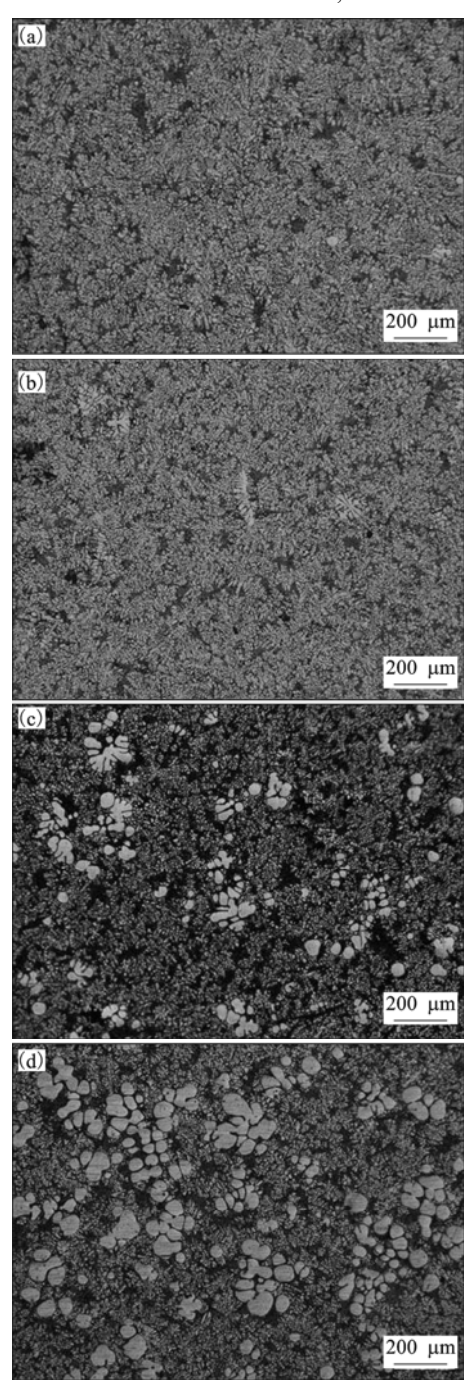


Fig.4 Microstructures of samples quenched after rheocasting time of 15 s (a), 17 s (b), 20 s (c) and 90 s (d)[28]

secondary or tertiary arms are detached by remelting at the roots due to solute enrichment and thermo-solutal convection near the dendrite roots[27, 29].

Following this mechanism, it can be explained that the cold graphite diffuser that is immersed in the melt with low superheat temperature causes numerous fine dendritic grains to nucleate and grow on the diffuser surfaces. These grains are quickly "pushed" out to the bulk liquid by the flow of gas bubbles. Most of these very fine "mother dendrite" grains will then be re-melted at the first few seconds of the rheocasting process since

the bulk liquid still consists of several small pools of superheated liquid. Only few disintegrated particles survive and are left in the melt as observed at the early time in Figs.4(a) and (b). After the superheat temperature is removed from the melt, more disintegrated particles can survive as observed at longer times in Figs.4(c) and (d). These fine particles will then grow and eventually coarsen to yield globular structure.

4 Applications of GISS process

The current focus of the GISS process is on forming semi-solid slurries containing low fractions solid (< 0.25) into parts even though the GISS process can also produce semi-solid metal containing higher fractions solid (0.3–0.6). The key reason for this choice is the prompt exploitation of the benefits of semi-solid metal in the casting industry since little modifications to the current machines and processing steps are required for this approach.

Several forming processes such as die casting, squeeze casting, gravity casting, and rheo-extrusion of the slurries prepared by the GISS process have been researched and developed for the past two years. In these forming processes, the added step is the immersion of graphite diffuser to inject gas bubbles for the duration of about 5–20 s. Semi-solid slurries containing up to 25% solid are then poured into shot sleeve holes, squeeze casting dies, sand molds, or extrusion shot holes for the GISS die casting, squeeze casting, sand casting, and rheo-extrusion, respectively. Fig.5 shows the schematic diagram of these GISS forming processes.

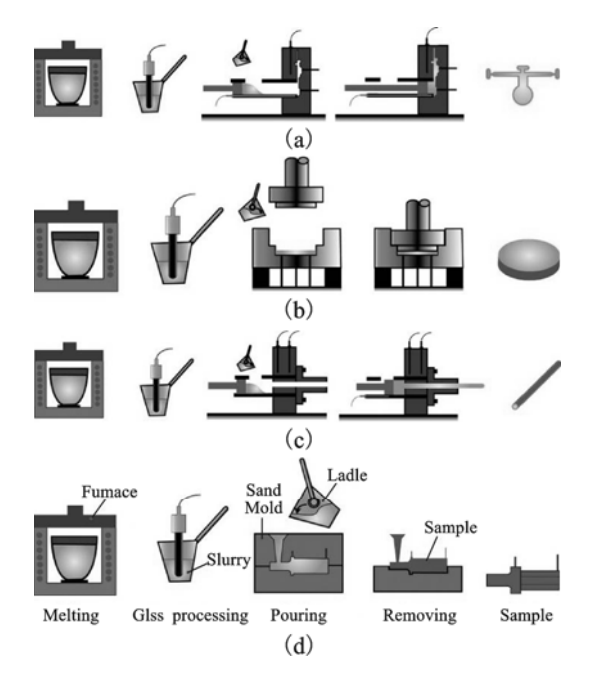


Fig.5 Schematic diagrams of GISS forming processes: (a) GISS die casting; (b) GISS squeeze casting; (c) GISS rheo-extrusion; (d) GISS low pressure casting

Various commercial alloys have been produced using the GISS process. Examples of the alloys, shown in Fig.6, include cast aluminum alloys, die casting

aluminum alloys, wrought aluminum alloys and zinc die casting alloys such as 356, A380, A383, 5052, 6061, 2024, 7075, and ZAMAK-3.

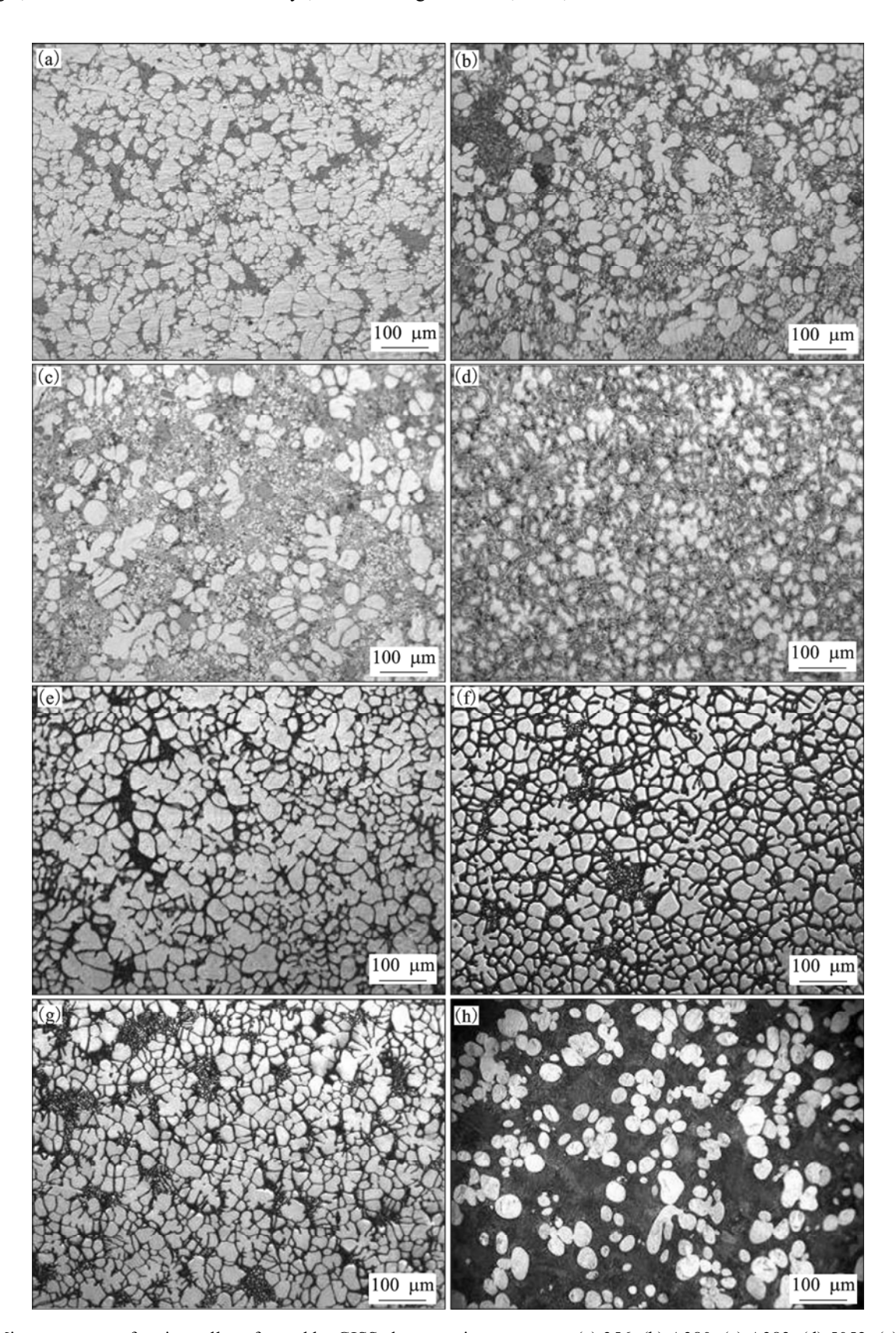


Fig.6 Microstructures of various alloys formed by GISS slurry casting processes: (a) 356; (b) A380; (c) A383; (d) 5052; (e) 6061; (f) 2024; (g) 7075; (h) ZAMAK-3

5 Development of industrial applications

The current industrial developments of the GISS process mainly involve the development of the GISS machines. The first versions of the machines used a handheld graphite diffuser to perform laboratory experiments (Fig.7(a)). Later, a semi-automatic machine (Fig.7(b)) was developed allowing a better control of the solid fractions to be produced. However, this machine still required manual ladling and pouring. Currently, an automatic version is developed to be used with a die casting machine. Fig.7(c) shows the prototype machine tested with an 80 t die casting machine.

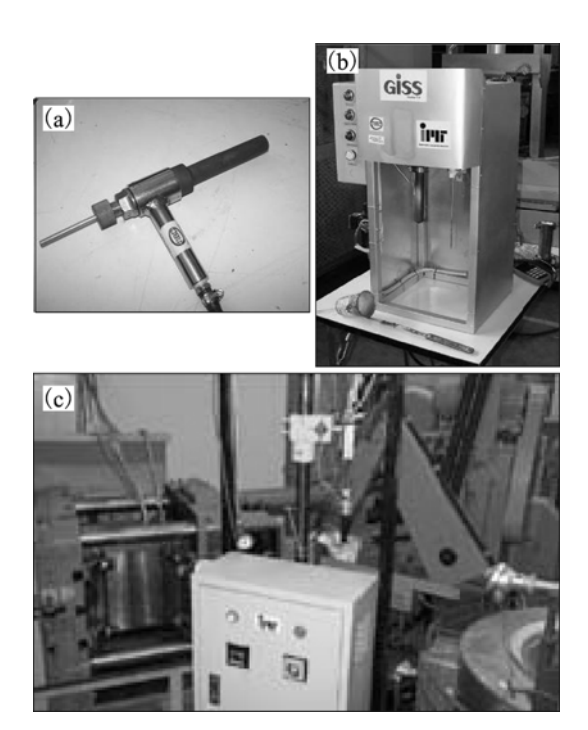


Fig.7 Different versions of GISS machines: (a) Handheld; (b) Semi-automatic; (c) Automatic

Currently, several commercial parts are being developed using the GISS process. Fig.8 shows some of these parts, which include an automotive rotor cover, a prosthesis tube adaptor, and a prosthesis foot adaptor. Other automotive and electronic applications are also considered. All the commercial activities are conducted by GISSCO, Co. Ltd.

6 Summary

This paper describes the gas induced semi-solid (GISS) process, which is developed in the industry. The process is currently focusing on producing low fractions solid for slurry casting processes. The GISS process requires minimal modifications to the machine and processing steps. It also allows the use of several currently

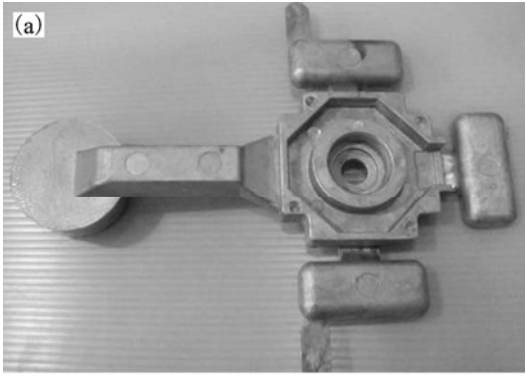






Fig.8 Examples of parts developed using GISS slurry die casting process: (a) Rotor cover; (b) Foot adaptor; (c) Tube adaptor

available alloys: both casting and wrought alloys. Currently, the process is developed for several commercial applications.

Acknowledgements

The authors would like to thank the financial supports from several sources including the Thai Research Fund (No. MRG5280215), Prince of Songkla University (No. AGR530031M), the Royal Golden Jubilee Ph.D. Program (No. PHD/0134/2551 and PHD/0173/2550), Prince of Songkla University for Ph.D. 50% Scholarship, the Materials Engineering Research Center, Western Digital, Mattel, the National Metal and Materials Technology Center (MTEC), and the National Science and Technology Development Agency (NSTDA).

The helps from the Innovative Metal Technology team, especially, Miss Buasang, Miss Chalinda, and Mr. Trinnamet are gratefully acknowledged. We also thank our collaborators, Dr. Pongsak Dulyapraphant, GISSCO Co., Ltd., and UMC Die Casting.

References

- LADOS D A, APELIAN D. Processing of Alloys and Composites[C]//. Proceedings of the 8th International Conference on Semi-solid. Limassol, Cyprsu, 2004.
- [2] KANG C G, KIM S K, LEE S Y. Processing of Alloys and Composites[C]//. Proceedings of the 9th International Conference on Semi-solid. Busan, Korea, 2006.
- [3] KNAUF F, BAADJOU R, HIRT G. Processing of Alloys and Composites[C]//. Proceedings of the 10th International Conference on Semi-solid. Aachen, Germany and Liege, Belgium, 2008.
- [4] UBE Industries Ltd. Method and apparatus for shaping semisolid metals. EPO 745694A1 [P]. 1996.
- [5] JORSTAD J, THIEMAN M, KAMM R. SLC, the newest and most economical approach to semi-solid Metal (SSM) casting [C]// The 7th International Conference on Semi-Solid Processing of Alloys and Composites. Tsukuba, Japan, 2002: 701–706.
- [6] YURKO J A, MARTINEZ R A, FLEMINGS M C. Development of the semi-solid rheocasting (SSR) process [C]// The 7th International Conference on Semi-solid Processing of Alloys and Composites. Tsukuba, Japan, 2002: 659–664.
- [7] FAN Z. Development of the rheo-discasting process for magnesium alloys [J]. Materials Science and Engineering A, 2005, 413/414: 72-78.
- [8] GRANATH O, WESSEN M, CAO H. Determining effect of slurry process parameters on semisolid A356 alloy microstructures produced by rheo metal process [J]. International Journal of Cast Metals Research, 2008, 21(5): 349–358.
- [9] HIRT G, KOPP R. Thixoforming-semi-solid metal processing [M]. Germany: Wiley-VCH, 2009.
- [10] WANNASIN J, MARTINEZ R A, FLEMINGS M C. Grain refinement of an aluminum alloy by introducing gas bubbles during solidification [J]. Scripta Materialia, 2006, 55(2): 115–118.
- [11] WANNASIN J, MARTINEZ R A, FLEMINGS M C. A novel technique to produce metal slurries for semi-solid metal processing [J]. Solid State Phenomena, 2006, 116: 366–369.
- [12] WANNASIN J, THANABUMRUNGKUL S. Development of a semi-solid metal processing technique for aluminium casting applications [J]. Songklanakarin Journal of Science and Technology, 2008, 30(2): 215–220.
- [13] WANNASIN J, JUNUDOM S, RATTANOCHAIKUL T, FLEMINGS M C. Development of the gas induced semi-solid metal

- process for aluminum die casting applications [J]. Solid State Phenomena, 2008, 141/142/143: 97–102.
- [14] KIRKWOOD D H, SUERY M, KAPRANOS P, ATKINSON H V, YOUNG K P. Semi-solid processing of alloys [M]. New York, Heidelberg, Dordrecht: Springer, 2009.
- [15] FLEMINGS M C. Behavior of metal alloys in the semisolid state [J]. Metallurgical Transactions B, 1991, 22B: 269.
- [16] FLEMINGS M C. Behavior of metal alloys in the semi-solid state [J]. Metallurgical Transaction A, 1991, 4: 957–981.
- [17] FLEMINGS M C, RIEK RG, YOUNG K P. Rheocasting processes [J]. AFS International Cast Metal Journal, 1976: 11–22.
- [18] KENNY M P, COURTOIS J A, EVANS R D, FARRIOR G M, KYONKA C P, KOCH A A, YOUNG K P. Metals handbook [M]. 9th Ed. Ohio: ASM International, 1988: 327.
- [19] TAUSIG G, XIA K. Thixoforming of a liquidus cast aluminum alloy [C]// The 5th International Conference on Semi-solid Processing of Alloys and Composites. Golden, Colorado, 1998: 473–480.
- [20] XIA K, TAUSIG G. Liquidus casting of a wrought aluminum alloy 2618 for thixoforming [J]. Materials Science and Engineering A, 1998, 246: 1–10.
- [21] ABRAMOV V O, ABRAMOV O V, STRAUMAL B B, GUST W. Hypereutectic Al-Si based alloys with a thixotropic microstructure produced by ultrasonic treatment [J]. Materials Design, 1997, 18(4/5/6): 323–326.
- [22] JIAN X, XU X, MEEK T T, HAN Q. Effect of power ultrasound on solidification of aluminum A356 alloy [J]. Materials Letters, 2005, 59: 190–193.
- [23] WANNASIN J, MARTINEZ R A, FLEMINGS M C. Method to prepare metal structure suitable for semi-solid metal processing. PCT/US2007/002 [P]. 2007.
- [24] DE FIGUEREDO A. Science and Technology of Semi-Solid Metal Processing [M]. Illinois: NADCA, 2001.
- [25] FLEMINGS M C. Solidification processing [M]. New York: McGraw-Hill Book Company, 1974.
- [26] MARTINEZ R A, FLEMINGS M C. Evolution of particle morphology in semisolid processing [J]. Metallurgical and Materials Transactions A, 2005, 36: 2205–2210.
- [27] FLEMINGS M C, YURKO J A, MARTINEZ R A. Solidification processes and microstructures [C]//A symposium in Honor of Wilfried Kurz as held at the 2004 TMS Annual Meeting. Charlotte, North Carolina, 2004: 3–14.
- [28] WANNASIN J, CANYOOK R, BURAPA R, FLEMINGS M C. Evaluation of solid fraction in a rheocast aluminum die casting alloy by a rapid quenching method [J]. Scripta Materialia, 2008, 59: 1091–1094.
- [29] JACKSON K A, HUNT J D, UHLMANN D R, SEWARD T P. On the origin of the equiaxed zone in casting [J]. Transaction of the Metallurgical Society of AIME, 1966, 236: 149–157.

(Edited by LI Xiang-qun)



Available online at www.sciencedirect.com



Trans. Nonferrous Met. Soc. China 20(2010) 1649-1655

Transactions of Nonferrous Metals Society of China

www.tnmsc.cn

Evolution of microstructure in semi-solid slurries of rheocast aluminum alloy

R. CANYOOK¹, S. PETSUT¹, S. WISUTMETHANGOON², M. C. FLEMINGS³, J. WANNASIN¹

- Department of Mining and Materials Engineering, Faculty of Engineering, Prince of Songkla University, Hat Yai, Songkhla, 90112, Thailand;
 Department of Mechanical Engineering, Faculty of Engineering, Prince of Songkla University, Hat Yai, Songkhla, 90112, Thailand;
- 3. Department of Materials Science and Engineering, Massachusetts Institute of Technology, Cambridge, MA 02139, USA

Received 13 May 2010; accepted 25 June 2010

Abstract: Semi-solid metal processing is being developed in die casting applications to give several cost benefits. To efficiently apply this emerging technology, it is important to understand the evolution of microstructure in semi-solid slurries for the control of the rheological behavior in semi-solid state. An experimental apparatus was developed which can capture the grain structure at different times at early stages to understand how the semi-solid structure evolves. In this technique, semi-solid slurry was produced by injecting fine gas bubbles into the melt through a graphite diffuser during solidification. Then, a copper quenching mold was used to draw some semi-solid slurry into a thin channel. The semi-solid slurry was then rapidly frozen in the channel giving the microstructure of the slurry at the desired time. Samples of semi-solid 356 aluminum alloy were taken at different gas injection times of 1, 5, 10, 15, 20, 30, 35, 40, and 45 s. Analysis of the microstructure suggests that the fragmentation by remelting mechanism should be responsible for the formation of globular structure in this rheocasting process.

Key words: microstructure evolution; rheocasting; rapid quenching method; 356 aluminum alloy; gas induced semi-solid (GISS); formation mechanism

1 Introduction

Semi-solid metal (SSM) processing has been used for about 40 years in the metal casting industry to produce higher quality parts than conventional die casting with lower cost than forging processes. Two SSM processing routes are used industrially: thixocasting and rheocasting. Thixocasting can yield high-quality parts with high mechanical properties. However, the costs of the aluminum feedstock billets, reheating system, and forming machines are quite high. However, the recent trend in semi-solid metal processing is focused on applying the rheocasting route[1]. This is because rheocasting can offer cost advantages over thixocasting. In this SSM route, liquid alloy is processed into semi-solid metal at the production site and scrap metals can be recycled in-house[1].

To efficiently apply the rheocasting process, it is important that the quality of the slurry is carefully controlled during the production. In addition, it is desirable that the process is efficient in producing semi-solid metal in a short time with homogeneous and globular microstructure[2]. To achieve these requirements, it is important to understand the mechanism of the formation of globular structure during rheocasting processes.

In literatures, it is well accepted that the globular microstructure is obtained when a large number of solid grains are formed during the early stages of solidification[3]. The high density of the solid grains results in non-dendritic growth and, therefore, globular microstructure is achieved. However, it is still unclear how these numerous solid grains are formed[4].

Two theories are often proposed by many researchers: copious nucleation and fragmentation. Some researchers[5–9] proposed that the globular grains form directly through direct nucleation and growth. Others[10–14] proposed that the grains come from fragmented dendrite arms. These previous studies in the literatures[5–14] confirm that there are still disagreements among the researchers regarding the

mechanism responsible for forming the numerous solid grains in the semi-solid microstructure. In order to understand the formation mechanism, it is important to study the microstructure evolution at the early stages.

This work aims to investigate the microstructure evolution during the early stages of solidification using a rapid quenching mold technique previously used by several investigators[1].

2 Theory

Two mechanisms that are often proposed to explain the formation of a high density of solid particles are copious nucleation and fragmentation.

2.1 Copious nucleation mechanism

This mechanism proposes that the numerous grains are obtained as a result of copious nucleation that is achieved by rapid and continuous heat extraction and melt convection. Crucible walls, cold immersed solid surfaces, or inoculant surfaces provide effective heterogeneous nucleation sites for the solid grains to form. Grain nucleation requires a minimum amount of undercooling to be effective so most potential nucleation sites become inactive when the local temperature rises due to the release of latent heat from the previously nucleated grains nearby. As a consequence, only a small fraction of nuclei are formed[4]. Rapid and continuous heat extraction near these surfaces helps to remove the released latent heat, consequently, allowing more nuclei to form. Some of the literatures supporting this mechanism are as follows.

Researchers at C.I.T.[6] investigated a new semi-solid casting process for Cu-Sn alloys using an inclined cooling plate. They proposed the crystal separation theory, explaining that the granular crystals nucleate and grow on the chill mold wall and separate from it due to the fluid motion. The theory is shown schematically in Fig.1. LI et al[7] investigated the morphological evolution during solidification under stirring of succinonitrile-5% water (molar fraction) by in situ observation. They reported that the globular crystals form through direct nucleation and growth from the stirred melt when the alloy is cooled and stirred from a temperature above the liquidus or between the liquidus and solidus. WU et al[8] created semi-solid metal of an Al-Si alloy by introducing mechanical vibration during isothermal holding for 5 min. They suggested that numerous nuclei formed in the melt because of undercooling. Also, many nuclei formed on the crucible wall and then were transported into the bulk melt. JIAN et al[9] evaluated the effect of ultrasonic vibration on the nucleation and growth of aluminum alloy A356 melt. They concluded that the dominant mechanism for the

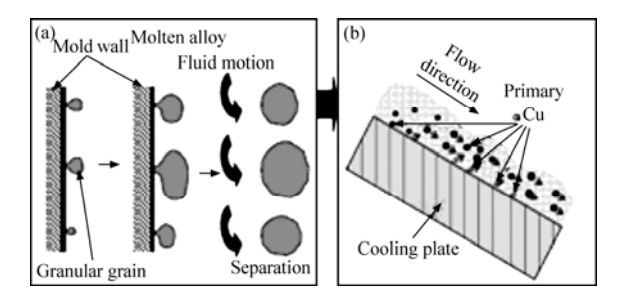


Fig.1 Schematic of crystal separation theory (a) and principle of generation of new semi-solid slurry using inclined cooling plate (b)[6]

formation of a globular microstructure was likely not due to the fragmentation mechanism, but heterogeneous nucleation induced by cavitation.

2.2 Fragmentation mechanism

This mechanism proposes that the high density of solid grains is created from detached secondary or tertiary arms due to solute enrichment and thermo-solutal convection near the dendrite root. FLEMINGS et al[10] suggested that vigorous stirring and localized rapid cooling can provide significant temperature disturbances in a molten metal, which is helpful for the remelting and separation of dendrite arms from a "mother" dendrite. This action as illustrated schematically in Fig.2 leads to grain multiplication. Some of the researches that support this mechanism are as follows.

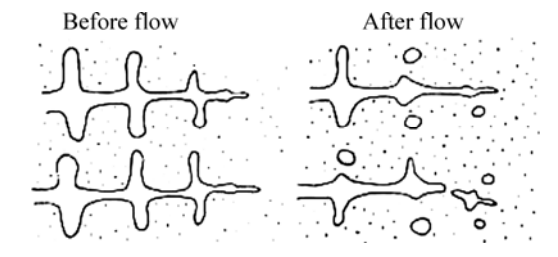


Fig.2 Schematic diagram of dendrite multiplication[10]

HELLAWELL et al[11] presented a detailed discussion on dendrite fragmentation and the effects of fluid flow in casting. They proposed that remelting of dendrite arms at their roots, rather than breaking off by a mechanical force, might be the cause of grain multiplication. JACKSON et al[12] found that the high solute concentration in the boundary adjacent to the primary phase will lower the local melting temperature. If the solute concentration is changed by the flow, the local melting temperature will be lowered and remelting may occur. JI[13] investigated the dendrite fragmentation in Sn-15%Pb (mass fraction) alloy under shearing using a twin-screw extruder. He suggested that the dendrites are fragmented via the penetration of liquid into the bent

dendrite arms to form large angle grooves along grain boundaries. Later, RUVALCABA et al[14] applied high-brilliance synchrotron X-radiation microscopy and image processing for in situ observations of local solute-enrichment during fragmentation of dendrite arms. The study was done under normal non-forced convection conditions during directional solidification of an Al-20% Cu (mass fraction) alloy. They found that local fragmentation is initiated by transient growth conditions. This occurs naturally during solidification, in which the solute is transported into the mush by gravity-induced liquid flow.

3 Experimental

The commercial 356 aluminium alloy was used in this study. The chemical composition of this alloy is given in Table 1. The liquidus temperature of the alloy is 613 °C, and the eutectic temperature is 573 °C.

Table 1 Chemical composition of 356 aluminium alloy in this study (mass fraction, %)

Si	Fe	Cu	Mn	Mg	Zn	Ti	Ni	Al
6.90	0.41	0.05	0.04	0.42	0.01	0.10	0.01	Bal.

Approximately 2 kg of the alloy was melted in a graphite crucible at 720 °C. A stirring impeller inserted at the bottom of the crucible was used at a low speed (<100 r/min) to homogenize the temperature of the melt in the crucible. Five thermocouples were used to record the temperatures at various positions as illustrated in Fig.3. The temperature data were recorded using Winview software through a data acquisition board. The gas induced semi-solid (GISS) process was used to create semi-solid slurry. In the GISS rheocasting process, a graphite diffuser was immersed into a molten metal held at a temperature above the liquidus temperature. In this work, the starting rheocasting temperature was 620 °C. Nine levels of solid fractions were obtained by varying rheocasting times (t_R) of 1, 5, 10, 15, 20, 30, 35, 40 and 45 s. To capture the instant microstructure, the rapid quenching method was used. This method had been previously used in several studies[1]. The rapid quenching mold is shown schematically in Fig.3. The high cooling rates achieved by the mold allowed the capture of the microstructure at a temperature. The channel thickness of the quenching mold of 1 mm was used for the short rheocasting times of 1, 5, 10, 15, 20, and 30 s. Longer rheocasting times of 35, 40, and 45 s yielded the semi-solid slurry with the viscosity too high that the quenched samples mostly consisted of segregated liquid phase. Thus, the channel thickness of the quench mold was increased to 3 mm to obtain

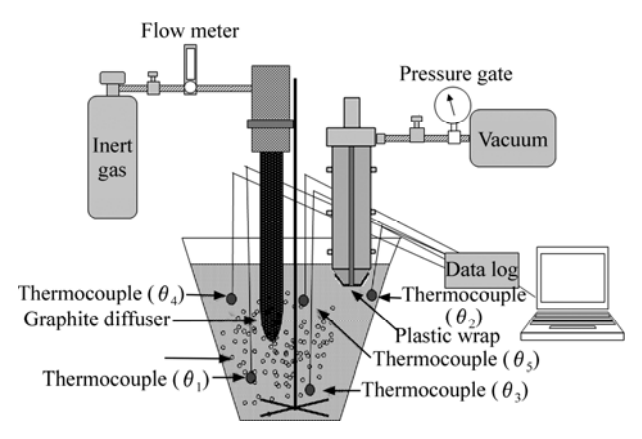


Fig.3 Schematic diagram of experimental setup

homogeneous semi-solid samples. For each rheocasting time, 3 samples were obtained for further analysis.

Metallographic examination of the quenched samples was performed at the top, middle and bottom locations of the quenched plates, as illustrated in Fig.4. Standard grinding and polishing processes were conducted. The samples were then etched with 2% HF water solution for 9–12 s. The microstructure of the samples was captured using an optical microscope equipped with an image acquisition system. An image processing software was used to adjust the brightness and contrast of the captured micrographs. Quantitative image analysis was then performed on the micrographs using Image Tool software.



Fig.4 Quenched plate and sample locations

4 Results and discussion

Representative sets of temperature distribution in the experiments are given in Table 2. For example, for the rheocasting time of 10 s, the temperatures at different locations in the melt are 614.3, 615.6, 615.9, 616.2 and 613.0 °C. The results show that the temperatures at different locations are not exactly the same. There are still pools of liquid metal with different temperatures even though agitation is applied to the melt.

Representative microstructures of the samples obtained at different rheocasting times are shown in Fig.5.

Observation on the microstructure shows that a mixture of globular, equiaxed, and dendritic particles are dispersed in the microstructure. The results in Table 2

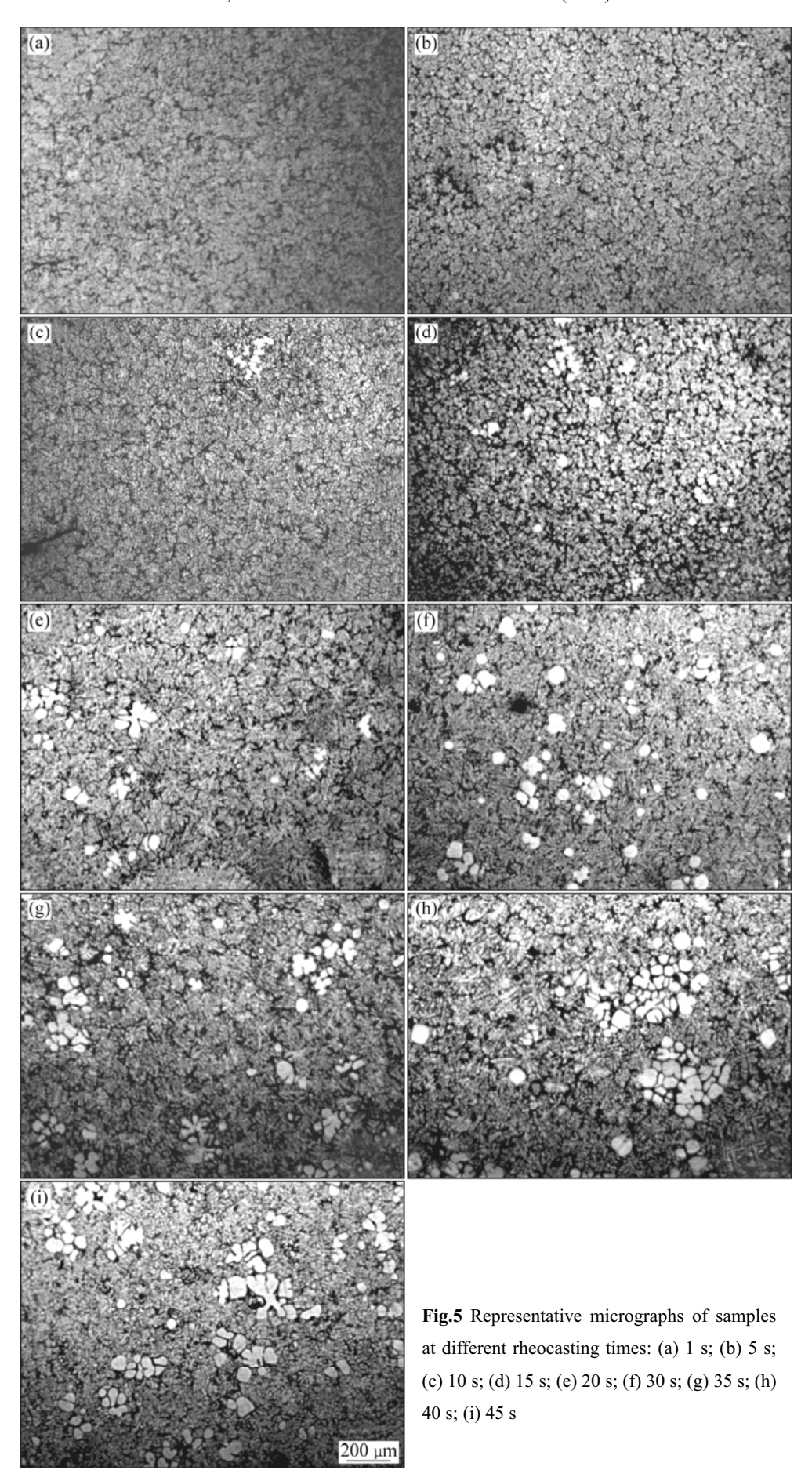


Table 2 Solid fractions and representative temperature distribution in slurry at different rheocasting times

Rheocasting	Tempe	Average				
time/s	θ_1	θ_2	θ_3	θ_4	θ_5	solid
tillie/ 5	01	02	03	04	o_5	fraction/%
1	619.2	620.6	618.7	620.7	620.2	0
5	619.3	620.3	620.8	618.4	617.8	0.01
10	614.3	615.6	615.9	616.2	613.0	0.05
15	611.5	612.5	611.8	611.4	611.9	2.05
20	610.1	612.3	610.1	611.7	611.6	2.78
30	612.5	613.4	612.1	612.5	611.9	5.55
35	611.5	607.4	608.7	609.8	609.0	7.89
40	609.1	604.0	606.5	603.1	602.8	10.86
45	608.9	602.2	606.3	603.5	602.7	14.58

show the final solid fractions of 0, 0.01%, 0.05%, 2.05%, 2.78%, 5.55%, 7.89%, 10.86% and 14.58% for the rheocasting times of 1, 5, 10, 15, 20, 30, 35, 40 and 45 s, respectively. The solid fraction increases as the rheocasting time increases as expected, since cooling is continually achieved, resulting in reduced temperatures, thus, increased solid fractions.

4.1 Effect of rheocasting time on particle density

The number of solid particles analyzed by quantitative image analysis as a function of the rheocasting time is summarized in Fig.6. The number of solid particles per square millimeter is 0, 0, 1, 11, 12, 25, 31, 36 and 47 for the rheocasting time of 1, 5, 10, 15, 20, 30, 35, 40 and 45 s, respectively. From these results, it can be noted that during the early rheocasting times of 1, 5 and 10 s, there are only a few solid particles in the melt. However, when the rheocasting time reaches 15 s, a significant increase in the solid particle density is obtained (from 1 to 11 mm⁻²). After that, the increase in the solid particle density is quite steady.

This interesting result may be explained by the fragmentation mechanism that once the cold graphite diffuser is inserted into the melt held at a temperature

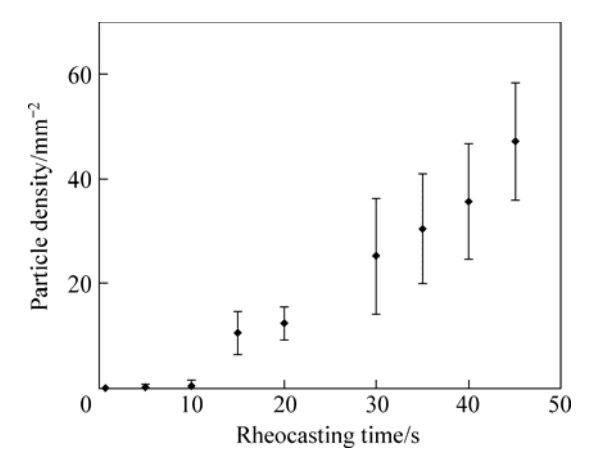


Fig.6 Effect of rheocasting time on particle density

slightly above the liquidus temperature, a large number of fine dendritic grains will be created near the cold surfaces and pushed away into the bulk liquid by the gas bubbles. During the early time of 1-10 s, the melt temperatures are still above the liquidus temperature. Thus, these mother dendrites will be remelted. However, remelting will take some time and there may be some pockets of undercooled liquid in the melt. So, there are some disintegrated or fragmented dendrite arms left in the melt as shown in the micrographs in Figs.5(a)-(c) even though the temperatures in the melt are above the liquidus temperature. When all the regions of the melt are not superheated (at the rheocasting times of 15 s and longer, see Table 2), a lot more fragmented arms from the remelting action can survive in the melt as observed in Fig.5(d). This action of remelting that yields the microstructure shown in Fig.5(d) can be explained schematically in Fig.2.

4.2 Effect of rheocasting time on spherical particle density

Close examination of the microstructure indicates that there are a lot of fine spherical particles in the mixture of equiaxed and dendritic particles. Fig.7 gives representative microstructures showing the spherical particles. From the quantitative analysis, the average number of spherical particle per square millimeter is 0, 0, 0.20, 2.27, 2.66, 3.80, 3.81, 3.83 and 3.75 for the rheocasting time of 1, 5, 10, 15, 20, 30, 35, 40 and 45 s,

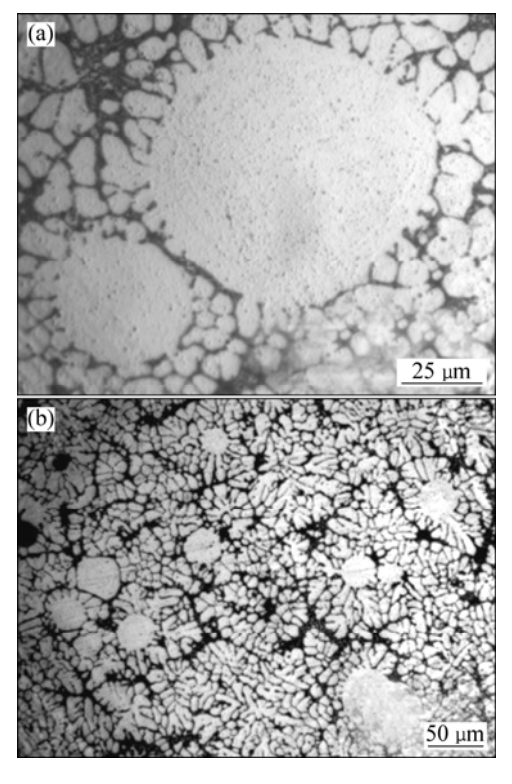


Fig.7 Representative microstructures of spherical particles: (a) In high magnification; (b) In low magnification

respectively. These results are also plotted in Fig.8. It can be noticed that the spherical particle density also significantly increases from the rheocasting time of 10 to 15 s. The increase continues until the rheocasting time of 30 s. After this time, the number of spherical particles appears to be roughly constant. These experimental results may be explained by the fragmentation mechanism.

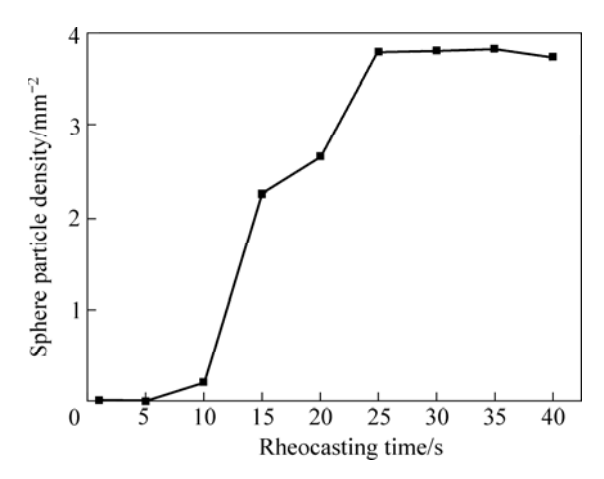


Fig.8 Effect of rheocasting time on spherical particle density

The fragmentation by remelting mechanism suggests that some spheroidal particles will definitely be created at the early stages from the detached secondary or tertiary dendrite arms. The schematic of this mechanism shown in Fig.2 predicts that the microstructure after fragmentation by remelting should consist of a mixture of dendritic, equiaxed and globular particles. A coarsening model, shown in Fig.9, also suggests the formation of spheroidal particles after a remelting event.



Fig.9 Dendrite coarsening model[16]

Sintering and coalescence of solid particles also occur in the slurry. During the fluid flow, solid particles may hit one another and sinter together. Fig.10 shows clumps of sintered particles. This phenomenon may explain why the spherical particle density remains constant as the rheocasting time increases. Although fragmentation may continue, yielding more spheroidal particles, the particles may be sintered together to form non-spherical clumps of particles. As the solid fraction increases, the chance for coalescence of particles is greater. Fig.11 shows examples of sintered particles that

are observed in the later rheocasting times in this work. Thus, from the results, it may be concluded that fragmentation of dendrite arms is continuously active in the early stages of the rheocasting process.



Fig.10 Clumps of sintered particles[17]

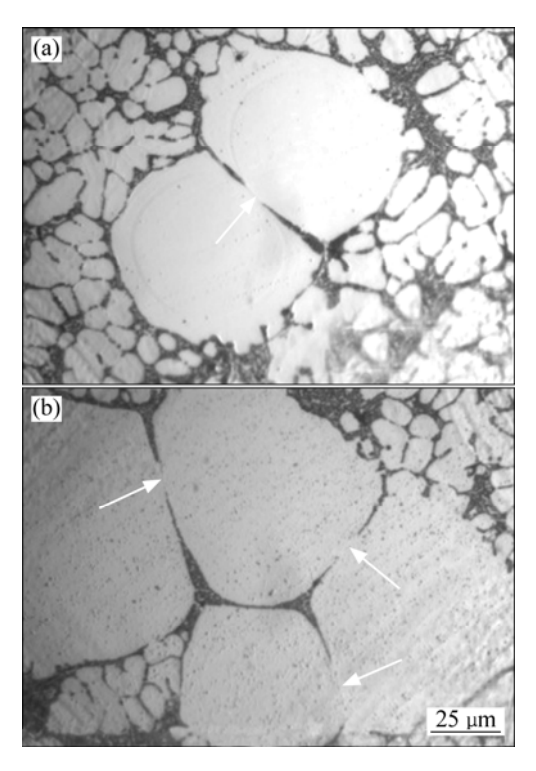


Fig.11 Examples of sintered particles (Arrows indicate weld joints)

5 Conclusions

- 1) The microstructure at the early stages of a rheocasting process consists of a mixture of spheroidal, equiaxed and dendritic particles.
- 2) During the early rheocasting times, a few solid particles are observed in the melt even though the temperature in the melt is higher than the liquidus temperature. This may be because of incomplete remelting of the dendrites formed by the rheocasting process. After all the temperatures in the melt decrease below the liquidus temperature, significantly more solid grains can survive and are present.

- 3) The density of spherical particles increases as the rheocasting time increases and remains constant after a certain rheocasting time. The results suggest that the fragmentation by remelting mechanism is responsible for producing the observed spherical particles. The reason for the constant spherical particle density may be because of particle sintering when the solid fraction is increased.
- 4) The rapid quenching mold technique can be used to study the microstructure evolution of semi-solid slurries at the early stages. The information obtained may give more understanding in the formation mechanism of semi-solid metal microstructure.

Acknowledgements

This work is funded by the Thai Research Fund (Contract No. MRG5280215) and the Royal Golden Jubilee Ph.D. Program (Grant No. PHD/0134/2551). The authors thank Mr. Songyot Jantawadee and the Innovative Metal Technology team for helping with the experiments and data analysis.

References

- JORSTAD J L. SSM processes An over view[C]//The 8th International Conference on Semi-Solid Processing of Alloys and Composites. Limassol, Cyprus, 2004.
- [2] KIRKWOOD D H, SUERY M, KAPRANOS P, ATKINSON H V, YOUNG K P. Semi-solid processing of alloys [M]. New York: Springer Heidelberg Dordrecht, 2009.
- [3] WANNASIN J, CANYOOK R, BURAPA R, FLEMINGS M C. Evaluation of solid fraction in a rheocast aluminum die casting alloy by a rapid quenching method [J]. Scripta Materialia, 2008, 59: 1091-1094.
- [4] de FIGUEREDO A. Science and technology of semi-solid metal processing [M]. Rosemont: The North American Die Casting Association, 2001.

- [5] IQBAL N, VAN DIJK N H, OFFERMAN S E, MORET M P, KATGERMAN L, KEARLEY G J. Real-time observation of grain nucleation and growth during solidification of aluminum alloys [J]. Acta Materialia, 2005, 53: 2875–2880.
- [6] C.I.T, MOTEGI T, TANABE F. New semi-solid casting of copper alloys using an inclined cooling plate [C]//The 8th International Conference on Semi-Solid Processing of Alloys and Composites. Limassol, Cyprus, 2004.
- [7] LI T, LIN X, HUANG W. Morphological evolution during solidification under stirring [J]. Acta Materialia, 2006, 54: 4815–4824.
- [8] WU S, XIE L, ZHAO J, NAKAE H. Formation of non-dendritic microstructure of semi-solid aluminum alloy under vibration [J]. Scripta Materialia. 2008. 58: 556-559.
- [9] JIAN X, XU H, MEEK T T, HAN Q. Effect of power ultrasound on solidification of aluminum A356 alloy [J]. Materials Letters, 2005, 59: 190-193
- [10] FLEMINGS M C, YURKO J, MARTINEZ R. Semi-solid forming: Our understanding today and its implications for improved process [C]//The 8th International Conference on Semi-Solid Processing of Alloys and Composites. Limassol, Cyprus, 2004.
- [11] HELLAWELL A, KIRKWOOD D H, KAPRANOS P. [C]// The Fourth International Conference on Semi-solid Processing of alloys and Composites. Sheffield: University of Sheffield, 1996: 40.
- [12] JACKSON K A, HUNT J D, UHLMANN D R, SEWARD T P. On the origin of the equiaxed zone in casting [J]. Transactions of the Metallurgical Society of AIME, 1966, 236: 149.
- [13] JI S. The fragmentation of primary dendrites during shearing in semisolid processing [J]. Materials Science, 2003, 38: 1559–1564.
- [14] RUVALCABA D, MATHIESEN R H, ESKIN D G, ARNBERG L, KATGERMAN L. In situ observations of dendritic fragmentation due to local solute-enrichment during directional solidification of an aluminum alloy [J]. Acta Mater, 2007, 55: 4287–4292.
- [15] MARTINEZ R A, FLEMINGS M C. Evolution of particle morphology in semi-solid processing [J]. Metallurgical and Materials Transactions A, 2005, 36: 2205–2210.
- [16] FLEMINGS M C. Solidification processing [M]. New York: McGraw-Hill Book Company, 1974.
- [17] NAFISI S, GHOMASHCHI R. The microstructural characterization of semi-solid slurries [J]. JOM, 2006, 58: 24–30.

(Edited by YANG Bing)



Available online at www.sciencedirect.com



Trans. Nonferrous Met. Soc. China 20(2010) 1756-1762

Transactions of Nonferrous Metals Society of China

www.tnmsc.cn

Feasibility of semi-solid die casting of ADC12 aluminum alloy

S. JANUDOM¹, T. RATTANOCHAIKUL¹, R. BURAPA², S. WISUTMETHANGOON³, J. WANNASIN¹

- 1. Department of Mining and Materials Engineering, Faculty of Engineering, Prince of Songkla University, Hat Yai, Songkhla, 90112, Thailand;
- 2. Department of Industrial Engineering, Faculty of Engineering, Rajamangala University of Technology Srivijaya, Songkhla, 90000, Thailand;
 - 3. Department of Mechanical Engineering, Faculty of Engineering, Prince of Songkla University, Hat Yai, Songkhla, 90112, Thailand

Received 13 May 2010; accepted 25 June 2010

Abstract: The feasibility of semi-solid die casting of ADC12 aluminum alloy was studied. The effects of plunger speed, gate thickness, and solid fraction of the slurry on the defects were determined. The defects investigated are gas and shrinkage porosity. In the experiments, semi-solid slurry was prepared by the gas-induced semi-solid (GISS) technique. Then, the slurry was transferred to the shot sleeve and injected into the die. The die and shot sleeve temperatures were kept at 180 °C and 250 °C, respectively. The results show that the samples produced by the GISS die casting give little porosity, no blister and uniform microstructure. From all the results, it can be concluded that the GISS process is feasible to apply in the ADC12 aluminum die casting process. In addition, the GISS process can give improved properties such as decreased porosity and increased microstructure uniformity.

Key words: ADC12 aluminum alloys; semi-solid die casting; gas induced semi-solid (GISS); rheocasting

1 Introduction

For many years aluminum parts have been used in several applications such as automotive, electronic, aerospace, and construction fields. These parts are generally produced in a large quantity by the high pressure die casting process. Several advantages of die casting process have been realized such as high production rate and the ability to form small complex parts. The die casting process involves the injection of liquid aluminum into a die cavity under high pressures. The metal stream "sprays" into the die cavity, causing metal reaction and air entrapment inside the casting. Therefore, the final parts have a structure which is full of gas bubbles and oxide inclusions. Furthermore, pressure die casting parts typically cannot be machined, anodized, welded, and heat treated because of these defects[1–4].

To improve the quality and properties of the die casting process, semi-solid metal technique has been introduced. A lot of semi-solid die casting studies have reported that using semi-solid die casting helps to improve the properties and increase the quality of die casting parts[5–7]. Semi-solid metal forming using the

rheocasting route can provide higher viscosity of the fluid. With the higher viscosity, less turbulent flow could be obtained, which helps to reduce air porosity and oxide inclusions during the die filling[5–7]. In addition, a rheocasting process can be easily applied with the conventional die casting process because the die casting machine only requires minor modifications[8].

Many research studies have shown successes in the semi-solid die casting with a rheocasting process[7–12]. However, most work have used the A356, A357, and ADC10 aluminum alloys. Despite ADC12 is used widely in the die casting industry, no complete research about semi-solid forming of this aluminum alloy has been published yet. The benefits of ADC12 aluminum alloy are good fluidity, excellent castability and high mechanical properties. In contrast, it is easy to have turbulent flow, which causes porosity defect, and it cannot normally be heat treated because of the surface the pore expansion high temperatures[13-14].

To solve the problems of ADC12 aluminum alloy, a semi-solid die casting process is selected to study in this work. The main objectives of this research are to study the feasibility of 1) the semi-solid processing of ADC12

aluminum alloy using the gas induced semi-solid (GISS) technique and 2) the semi-solid die casting of a commercial part.

2 Experimental

The material used in this study is commercial ADC12 aluminum alloy. The liquidus temperature of this alloy is 582 °C. The eutectic temperature of this alloy is 572 °C. The chemical composition measured using the optical emission spectrometer (OES) is shown in Table 1.

Table 1 Chemical composition of aluminum ADC12 alloy (mass fraction, %)

Si	Fe	Cu	Mn	Mg	Zn
11.88	0.93	1.75	0.12	0.07	0.78
	~	3.71		~	
Ti	Cr	Ni	Pb	Sn	Al

2.1 Semi-solid slurry preparation

In this experiment, an ADC12 aluminum alloy was melted in the graphite crucible in an electrical furnace at about 100 °C above the liquidus temperature (~680 °C). Approximately 200 g of the melt was taken from the crucible using a ladle. Next, the nitrogen gas was injected through a graphite diffuser into the ladle when the temperature of the melt was about 590 °C. The times to inject the gas were 5, 10 and 15 s. The schematic diagram of the GISS process is shown in Fig.1. At the varied injection times, the solid fractions were analyzed using the rapid quenching method. The high cooling rates achieved by the copper mold allow the capture of the microstructure at a certain temperature[15–16].

The microstructure of the samples from different rheocasting times was used to calculate the solid fraction. The Photoshop and Image Tool Software were used in the analysis[16].

2.2 Die casting process

The aluminum slurry prepared by the GISS process

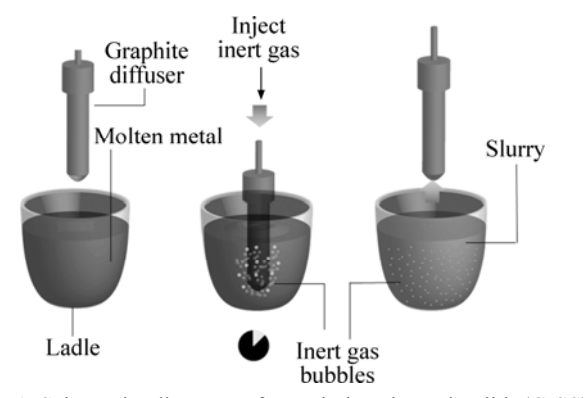


Fig.1 Schematic diagram of gas induced semi-solid (GISS) process

was transferred to the die casting machine. This machine has 80 t capacity for the clamping system. The slurry was poured into the shot sleeve kept at the temperature of 250 °C. The plunger forced the slurry into the die at various speeds of 0.05, 0.1 and 0.2 m/s. The die temperature was kept at 180 °C. The schematic diagram of the GISS die casting process is illustrated in Fig.2. In this study, the porosity, surface defect, surface blister, macro- and micro-structure of the samples were investigated. A summary of the parameters used in this study is illustrated in Table 2.

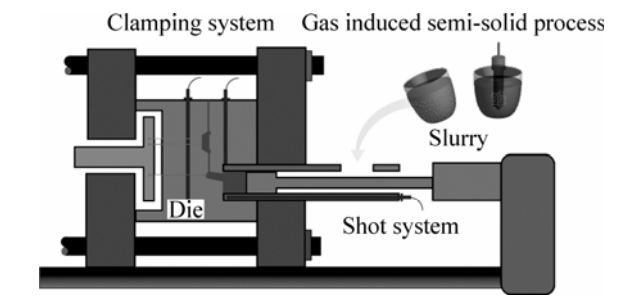


Fig.2 Schematic diagram of GISS die casting process

2.3 Die casting part analysis

The analysis methods are briefly described as follows.

1) Porosity analysis

The density of the sample (D_L) was measured using Eq.(1), and Eq.(2) was used to calculate the porosity (η) :

$$D_{\rm L} = \frac{m_{\rm dry}}{m_{\rm wet} - m_{\rm in-water}} \tag{1}$$

$$\eta = \frac{D_{\rm S} - D_{\rm L}}{D_{\rm S}} \tag{2}$$

where D_S is the standard density of an ADC12 aluminum alloy (2.76 g/cm³); D_L is the density from Eq.(1).

2) Surface defect and blistering test

Observation of the surface defect of the samples was conducted after the die casting process. The defects observed in this study were cold shut and blistering defects. The blistering was evaluated after the samples passed the solution treatment at 480 °C for 12 h.

3) Macro defects

All the samples were cut at the center as shown in Fig.3. Next, the samples were ground with the 320, 800, and 1200 grit papers to observe the macro defects.

4) Microstructure uniformity

The microstructure at different positions of the samples was observed using an optical microscope. The samples were cut and obtained from positions A, B, C, and D as shown in Fig.3. The samples were then prepared for metallographic analysis using standard grinding, polishing and etching procedures.

Table 2 Summary of parameters used in this study

Condition	Rheo-casting temperature/°C	Rheo-casting time/s	Gate thickness/ mm	Plunger speed/ (m·s ⁻¹)	Gate velocity/ (m·s ⁻¹)
Liquid	650	_	1.5	0.20	5.58
SSM1-1	590	5	3	0.20	2.79
SSM1-2	590	5	3	0.10	1.39
SSM1-3	590	5	3	0.05	0.69
SSM1-4	590	10	3	0.20	2.79
SSM1-5	590	10	3	0.10	1.39
SSM1-6	590	10	3	0.05	0.69
SSM1-7	590	15	3	0.20	2.79
SSM1-8	590	15	3	0.10	1.39
SSM1-9	590	15	3	0.05	0.69
SSM2-1	590	5	6	0.20	1.39
SSM2-2	590	5	6	0.10	0.69
SSM2-3	590	5	6	0.05	0.35
SSM2-4	590	10	6	0.20	1.39
SSM2-5	590	10	6	0.10	0.69
SSM2-6	590	10	6	0.05	0.35
SSM2-7	590	15	6	0.20	1.39
SSM2-8	590	15	6	0.10	0.69
SSM2-9	590	15	6	0.05	0.35

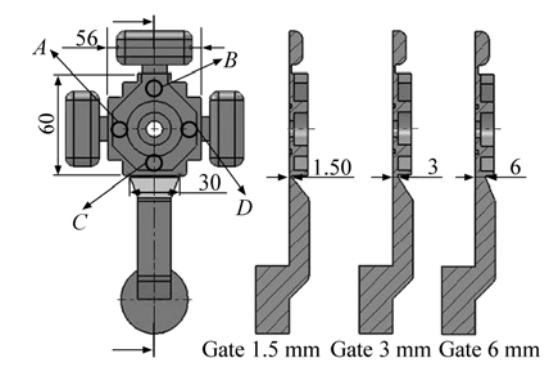


Fig.3 Drawing of increased rheocasting time part

3 Results and discussion

3.1 Semi-solid slurry

From the obtained results, the slurries produced by the conditions of the rheocasting times of 5, 10 and 15 s have the solid fractions of 0.25%, 6.33%, and 13.03%, respectively. The representative microstructures of the quenched samples at different rheocasting times are shown in Fig.4. The micrographs illustrate that amount of the primary $\alpha(Al)$ (white phase) increases with increased rheocasting time. The viscosity of the slurry should be increased when the solid fraction is increased.

It can be concluded that the ADC12 aluminum alloy can be produced into a semi-solid slurry at a desired solid fraction by varying the rheocasting time using the GISS process.

3.2 Die casting process

A representative sample produced by the semi-solid

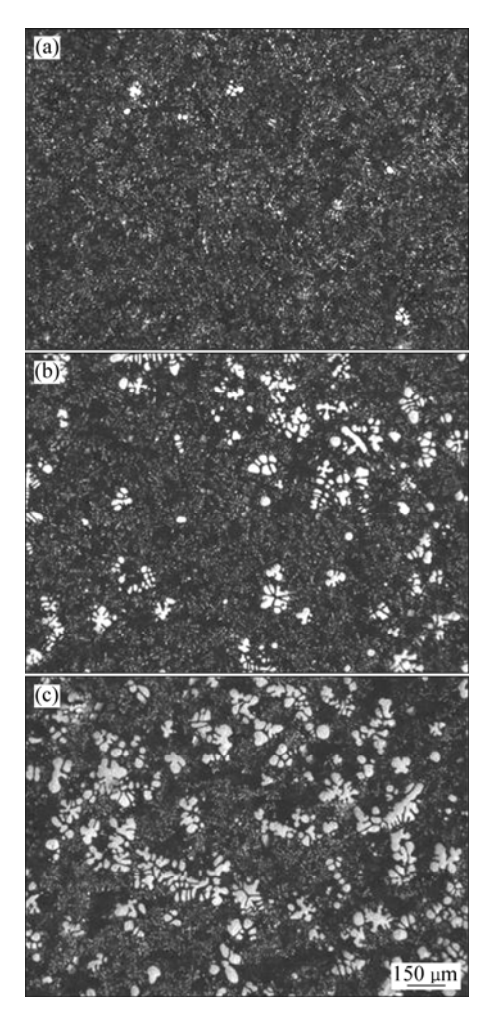


Fig.4 Representative micrographs of samples at different rheocasting times: (a) 5 s; (b) 10 s; (c) 15 s

die casting process is shown in Fig.5. The sample consists of three overflows, a runner, and a biscuit. Most samples had complete metal filling in the overflow and good surface finish. Only the samples produced with a higher solid fraction had the cold shut defect as shown in Table 3 and the representative samples with the cold shut defect is shown in Fig.6.

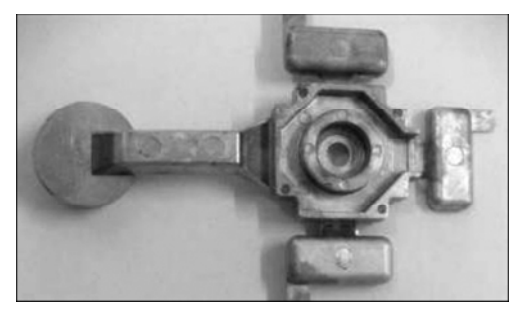


Fig.5 Representative picture of die casting part

The high solid fractions cause the viscosity of the slurry higher. For the thin gate (3 mm), the high viscosity slurry was difficult to flow into the die so that the metal could not fill the part completely. In addition, the cold shut defect was found because of the shorter solidification time of the higher solid fractions.

3.3 Porosity analysis

The results show that the samples produced by the

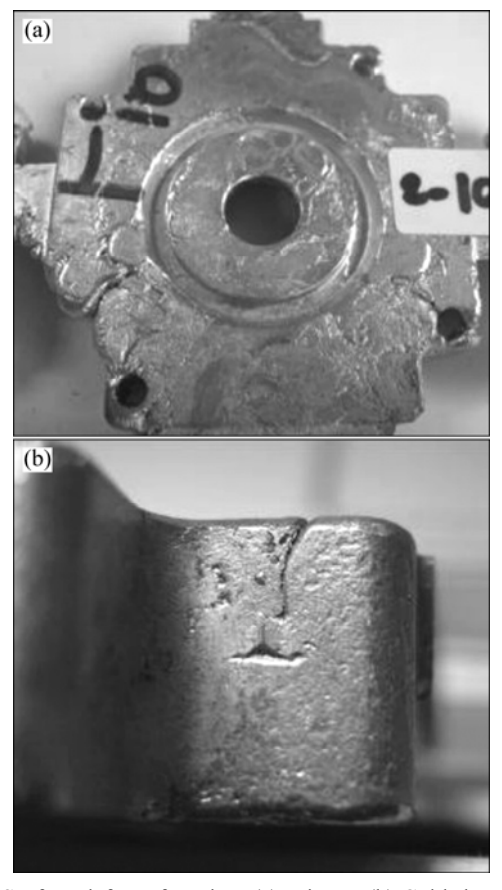


Fig.6 Surface defect of casting: (a) Misrun; (b) Cold shut

Table 3 Summary of die casting result

Condition	Solid fraction/%	Gate velocity/(m·s ⁻¹)	Porosity/%	Macrodefect	Blister	Note
Liquid	0	5.58	5.02	\checkmark	$\sqrt{}$	
SSM1-1	0.25	2.79	1.91	\checkmark	$\sqrt{}$	
SSM1-2	0.25	1.39	1.87	\checkmark	$\sqrt{}$	
SSM1-3	0.25	0.69	2.34	\checkmark	$\sqrt{}$	
SSM1-4	6.33	2.79	1.80	\checkmark	×	
SSM1-5	6.33	1.39	1.82	$\sqrt{}$	×	
SSM1-6	6.33	0.69	M	_	_	
SSM1-7	13.03	2.79	1.76	\checkmark	$\sqrt{}$	C
SSM1-8	13.03	1.39	1.72	\checkmark	$\sqrt{}$	C
SSM1-9	13.03	0.69	M	_	-	C
SSM2-1	0.25	1.39	2.11	×	$\sqrt{}$	
SSM2-2	0.25	0.69	2.05	×	$\sqrt{}$	
SSM2-3	0.25	0.35	1.65	×	×	
SSM2-4	6.33	1.39	1.62	×	×	
SSM2-5	6.33	0.69	1.76	×	×	
SSM2-6	6.33	0.35	1.47	×	×	
SSM2-7	13.03	1.39	1.54	×	×	
SSM2-8	13.03	0.69	1.72	×	$\sqrt{}$	C
SSM2-9	13.03	0.35	1.76	×	$\sqrt{}$	C

M is misrun and C is cold shut defect.

liquid die casting and the semi-solid die casting processes have the porosity of about 5% and 1.7%, respectively. The porosities of the samples produced by both processes are compared in Fig.7. However, in the semi-solid die casting samples, the result of the porosity of different conditions of gating size and velocity are not significantly different.

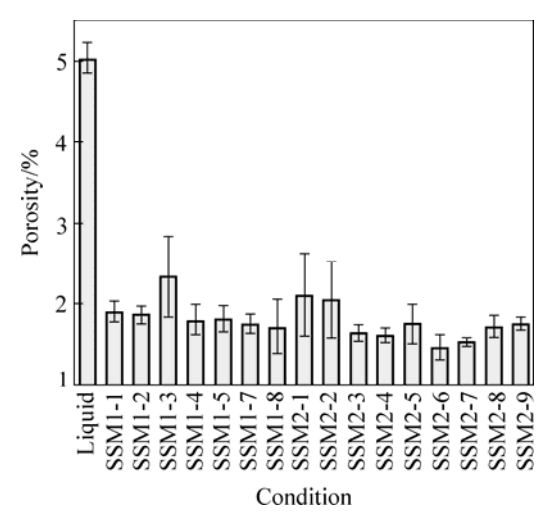


Fig.7 Porosity of samples under different conditions

In summary, in the liquid casting, turbulent flow is present, which results in porosity defect in the samples. In contrast, all the semi-solid die casting samples have lower porosity than the liquid die casting due to the less turbulent flow of the slurry. The larger gate also yields less porosity since it gives lower flow velocity.

3.4 Macrodefect analysis

All the samples produced by the semi-solid die casting with the thin gate have shrinkage porosity. In addition, gas porosity is found in the samples produced by the liquid die casting as shown in Table 3. The shrinkage porosity and gas porosity are shown in Fig.8. It can be concluded that the size of the gate has a large effect on the macro defects. The larger gate helps to reduce the turbulent flow and improve the feeding, which reduces the shrinkage porosity.

3.5 Surface blister

Surface blisters are found after the solution heat treatment process in about half of the samples. This defect is mostly found in the samples produced by the liquid die casting and the semi-solid die casting using a thin gates. In contrast, when the thick gate is employed for the semi-solid die casting, only the samples coded SSM2-8 and SSM2-9 have the defect, as shown in Table 3 and Fig.9.

In summary, the blister defect found in semi-solid die casting can be reduced by increasing the solid fraction and the gate size. However, the solid fraction

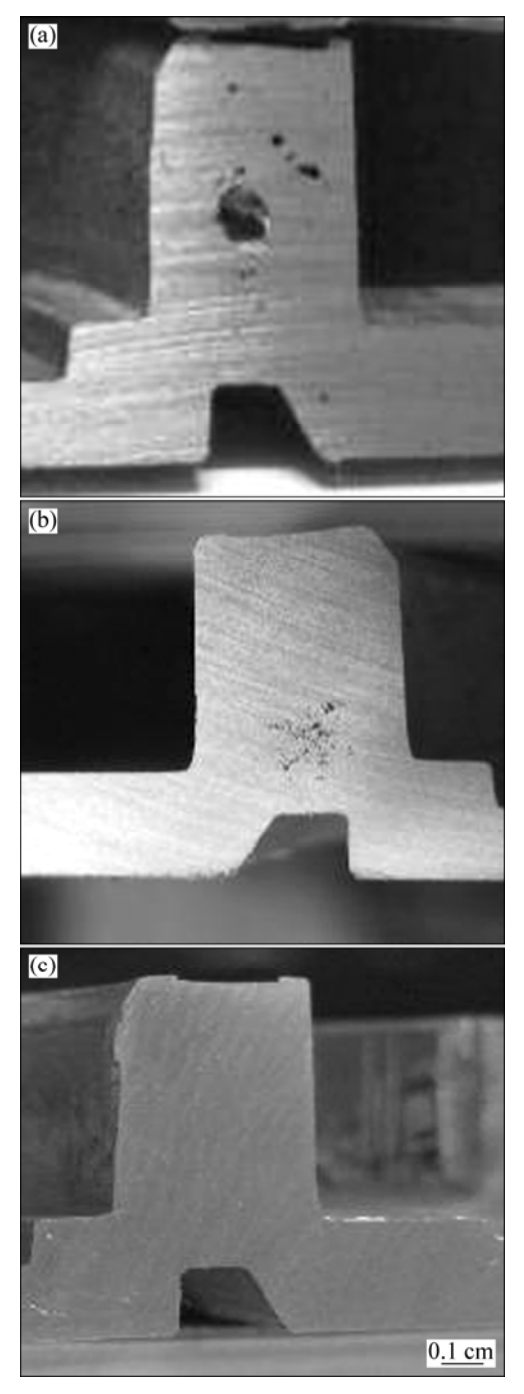


Fig.8 Macro views of cross section of samples: (a) Liquid die casting; (b) SSM1-1; (c) SSM2-6

should not be too high because it will be difficult to inject into the die.

3.6 Microstructure analysis

The representative microstructures of the samples produced by liquid die casting and semi-solid die casting are shown in Fig.10. Fine dendritic structure was observed in the samples from the liquid die casting process. However, in the samples from the semi-solid die casting process the microstructure consisted of primary α -phase, secondary α -phase and eutectic phase. The

primary α -phase structure was produced by the GISS process, then grew larger in the die. The secondary α -phase and eutectic structure were formed after the slurry flowed into the die. Because of the high cooling rates, the sizes of secondary α -phase and the eutectic

were very fine.

Observation of the microstructure uniformity at different positions is shown in Fig.11. The obtained micrographs illustrate that the microstructure at the positions A, B, C, and D are similar and uniform.

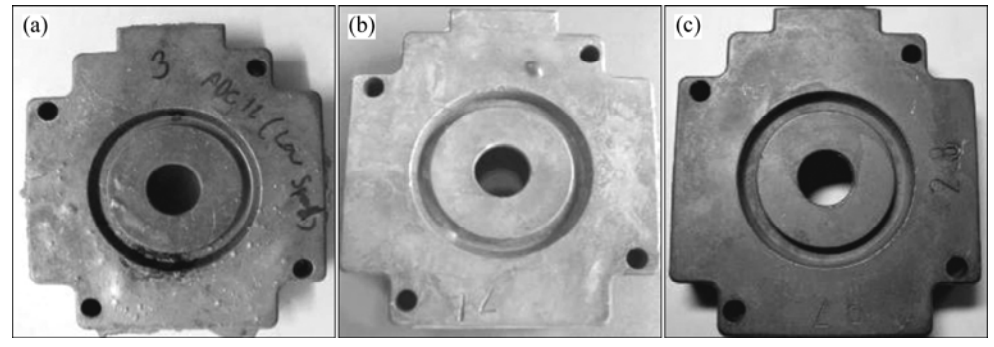


Fig.9 Surface blister in samples: (a) Liquid die casting; (b) SSM1-1; (c) SSM2-6

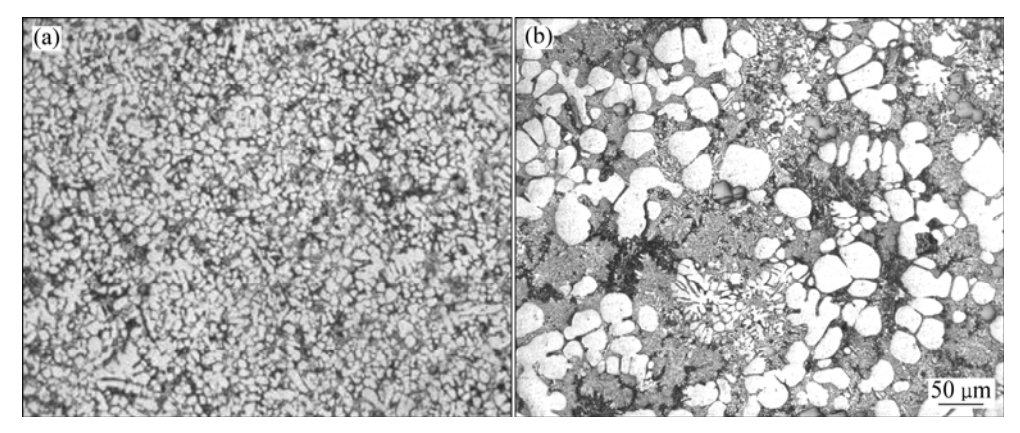


Fig.10 Microstructures of samples from liquid die casting (a) and semi-solid die casting (b)

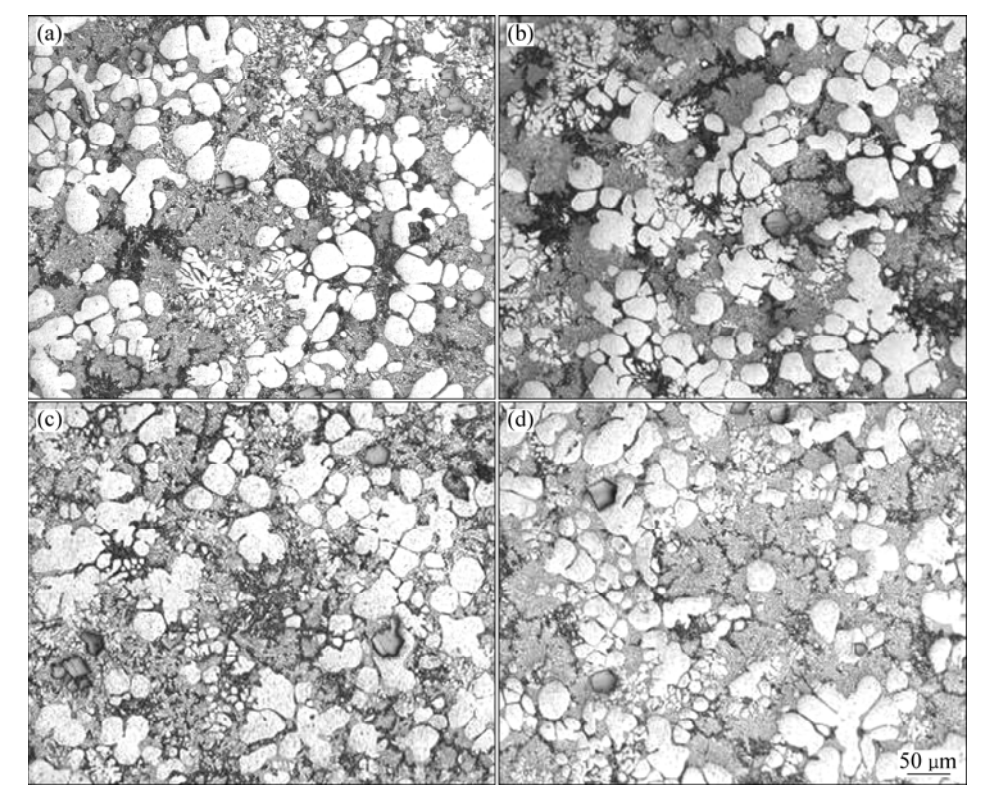


Fig.11 Representative microstructures at various positions of samples: (a) Point A; (b) Point B; (c) Point C; (d) Point D

4 Conclusions

- 1) It is feasible to produce semi-solid ADC12 parts using the gas induced semi-solid process.
- 2) The porosity and shrinkage defects in the parts can be reduced by increasing the solid fraction of the slurry.
- 3) Good casting parts of semi-solid die casting need appropriate plunger speeds and solid fractions of the slurry.
- 4) The microstructure of the produced samples is uniform throughout the casting parts.

Acknowledgements

This work is funded by the Royal Golden Jubilee Ph.D. Program (Grant No. PHD/0173/2550), the Thai Research Fund (Contract number MRG5280215) and Prince of Songkla University (Contract No. AGR530031M). The authors would like to thank the Innovative Metal Technology (IMT) team for kind support.

References

- [1] CAMPBELL J. Casting[M]. Oxford: Butterwort-Heinemann, 1991: 1–85.
- [2] ZHENG J, WANG Q, ZHAO P, WU C. Optimization of high-pressure die-casting process parameters using artificial neural network [J]. Advanced Manufacturing Technology, 2009, 44: 667–674.
- [3] VERRAN G O, MENDESB P K, ROSSIC M A. Influence of injection parameters on defects formation in die casting Al12Si13Cu alloy: Experimental results and numeric simulation [J]. Materials Processing Technology, 2006, 179: 190–195.
- [4] HANGAI Y, KITAHARA S. Quantitative evaluation of porosity in aluminum alloy die castings by fractal analysis of spatial distribution of area [J]. Materials and Design, 2009, 30: 1169–1173.

- [5] KIRKWOOD D H, SUERY M, KAPPANOR P, ATKINSON H V, YOUNG K P. Semi-solid processing of alloy [M]. New York: Springer, 2009.
- [6] FLEMING M C. Behavior of metal alloy in the semi-solid state [J]. Metallurgical Transaction A, 1991, 22: 957–981.
- [7] FAN Z, FANG X, JI S. Microstructure and mechanical properties of rheo-diecast (RDC) aluminium alloy [J]. Materials Science and Engineering A, 2005, 412, 298–306.
- [8] HONG C P, KIM J M. Development of an advanced rheocasting process and its applications [J]. Solid State Phenomena, 2006, 116/117: 44-53.
- [9] UBE Industries Ltd. Method and apparatus for shaping semi-solid metal: EPO 745694A1 [P]. 1996–12–04.
- [10] JORSTAD J, THIEMAN M, KAMM R. SLC: The newest and most economical approach to semi-solid metal (SSM) casting[C]//The 7th International Conference on Semi-solid Processing of Alloy and Composites. Tsukuba, Japan, 2002: 701–706.
- [11] YURKO J A, MARTINEZ R A, FLEMING M C. Development of the semi-solid rheocasting(SSR) process[C]//The 7th International Conference on Semi-solid Processing of Alloy and Composites, Tsukuba, Japan, 2002: 701–706.
- [12] WANNASIN J, JUNUDOM S, TATTANOCHAIKUL T, FLEMING M C. Development of the gas induced semi-solid metal process for aluminum die casting applications [J]. Solid State Phenomena, 2008, 141/142/143: 97–102.
- [13] TIANA C, LAMB J, van der TOUWC J, MURRAYA M, YAOD J Y, GRAHAMD D, JOHND D S T. Effect of melt cleanliness on the formation of porosity defects in automotive aluminium high pressure die castings [J]. Journal of Materials Processing Technology, 2002, 122: 82-93.
- [14] ZHAO H D, WANG F, LI Y Y, XIA W. Experimental and numerical analysis of gas entrapment defects in plate ADC12 die castings [J]. Materials Processing Technology, 2009, 209: 4537–4542.
- [15] WANNASIN J, CANYOOK R, BURAPA R, FLEMING M C. Evaluation of solid fraction in a rheocasting aluminum die casting alloy by a rapid quenching method [J]. Scripta Materialia, 2008, 159: 1091–1094.
- [16] MARTINEZ R A, FLEMING M C. Evolution of particle morphology in semi-solid processing [J]. Metallurgical Material Transactions A, 2005, 36: 2205–2210.

(Edited by YANG Bing)



Available online at www.sciencedirect.com



Trans. Nonferrous Met. Soc. China 20(2010) 1763-1768

Transactions of Nonferrous Metals Society of China

www.tnmsc.cn

Development of aluminum rheo-extrusion process using semi-solid slurry at low solid fraction

T. RATTANOCHAIKUL¹, S. JANUDOM¹, N. MEMONGKOL², J. WANNASIN¹

- 1. Department of Mining and Materials Engineering, Faculty of Engineering, Prince of Songkla University, Hat Yai, Songkhla, 90112, Thailand;
 - Department of Industrial Engineering, Faculty of Engineering, Prince of Songkla University, Hat Yai, Songkhla, 90112, Thailand

Received 13 May 2010; accepted 20 June 2010

Abstract: An aluminum extrusion process is mainly used to fabricate long tubes, beams and rods for various applications. However, this process has a high production cost due to the need for investment of high-pressure machinery. The objective of this work is to develop a new semi-solid extrusion process using semi-solid slurry at low solid fractions. A laboratory extrusion system was used to fabricate aluminum rods with the diameter of 12 mm. The semi-solid metal process used in this study was the gas induced semi-solid (GISS) technique. To study the feasibility of the GISS extrusion process, the effects of extrusion parameters such as plunger speed and solid fraction on the extrudability, microstructure, and mechanical properties of extruded samples were investigated. The results show that the plunger speed and solid fraction of the semi-solid metal need to be carefully controlled to produce complete extruded parts.

Key words: aluminum alloys; extrusion; semi-solid metal; rheo-extrusion; gas induced semi-solid (GISS)

1 Introduction

Extrusion is one of the various forming processes that is used to produce long and straight metal products with constant cross section, such as bars, solid and hollow sections, tubes, and wires[1]. In extrusion process, a billet is heated and forced through a die orifice. The products from this extrusion process are in a near net shape. However, the extrusion process requires a high-pressure machine to force the metal in the solid state. In addition, defects such as surface cracking, oxide inclusion and piping defect can be found in the products of an extrusion process[2].

An alternative way to reduce these process limitations is to apply a semi-solid extrusion process because it has several advantages such as the requirements of low extrusion force, good flowability, and less friction between the dies and the materials[3].

During the past several years, thixo-extrusion has been continuously developed since it is found to be able to achieve high quality products, for example, good surface finish and high ultimate tensile strength[4–10].

However, in a thixo-extrusion process, it is necessary to use a billet so only certain types of alloys can be processed and the scrap cannot be recycled on site[11]. From these restrictions, many research teams are focusing on the rheo-extrusion approach[12–16].

In previous studies on a rheo-extrusion process, FAN et al[12-13] performed experiments with twin screw rheo extrusion (TSRE) for magnesium alloys. The solid fractions produced in their work were more than 30% and the sleeve was kept at a high temperature of 630 °C and plunger speed was about 1 cm/s. The samples had uniform microstructure and quite high tensile strengths. LEE et al[14] investigated the behavior of melt extrusion for Al-Cu alloys. In the process, the molten Al-Cu alloy was held in a shot sleeve until the solid fraction was 78%. The slurry with the high solid fraction was then forced through the opening die at the plunger speed between 0.2 and 1.1 cm/s. The extrusion die was also kept at high temperatures of 500-520 °C. They reported that the high temperature of the die caused segregation of liquid phase. The way to solve this problem was to use lower die temperatures or to add some grain refiners.

In summary, from Refs.[12-14], most of the rheo-

extrusions used high solid fractions to produce the extruded products, and therefore they needed to use low ram speed and high temperature of the dies because of the high friction between the die and the materials.

The goal of this research is to develop a new rheo-extrusion process that can be used with lower temperatures of the die and the sleeve. In addition, it should be able to be used with higher speeds than conventional extrusion. Therefore, the process focuses to use semi-solid slurry with low solid fractions. A recent work in rheocasting using low solid fractions is published by WANNASIN et al[15]. In their work, semi-solid die casting at low solid fractions was developed using the gas induce semi-solid (GISS) process. Good properties such as low porosity and improved tensile properties were reported in their work. Thus, in this present work, the GISS technique is selected to be used with the rheo-extrusion process. And a preliminary research and development work of a new rheo-extrusion process using semi-solid slurry with low solid fractions employing the GISS technique is reported.

2 Experimental

2.1 Semi-solid rheo-extrusion experiments

The raw material used in this work was aluminum 356 alloy or JIS AC4C. The chemical composition of the alloy is shown in Table 1.

Table 1 Chemical composition of aluminum 356 alloy (mass fraction, %)

Si	Fe	Cu	Mn	Mg	Zn	Ti	Al
6.9	0.42	0.05	0.04	0.42	0.01	0.10	Bal.

In the experiments, the aluminum alloy was melted in an electric furnace at about 650 °C. Approximately 250 g of the molten aluminum was taken from the crucible by a ladle. When the temperature of the molten aluminum was about 620 °C, a graphite diffuser was immersed to produce the semi-solid slurry with the solid fractions of 5%, 10%, and 20%, respectively. A schematic drawing of the GISS technique is shown in Fig.1.

The semi-solid slurry from the GISS machine was then poured into a shot sleeve with the inner diameter of 40 mm. The shot sleeve was preheated to about 250 °C. Next, the slurry was forced by a plunger at various speeds of 2, 4, and 6 cm/s through a die, a graphite support and a water-cooled tube. The inner diameter of the die was 12 mm. The parameters used in this study are summarized in Table 2. The schematic drawing of this rheo-extrusion process is shown in Fig.2. The machine used in this study has a 80 t capacity with a hydraulic system.

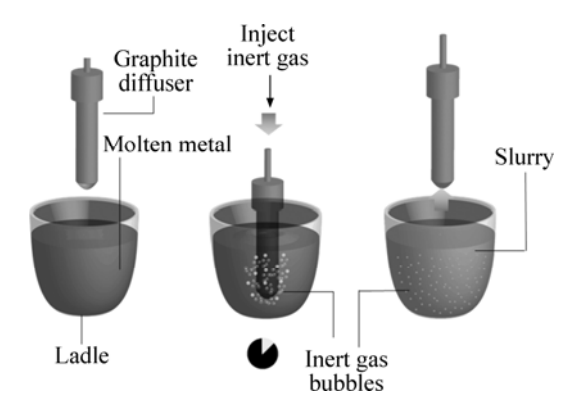


Fig.1 Schematic drawing of GISS technique

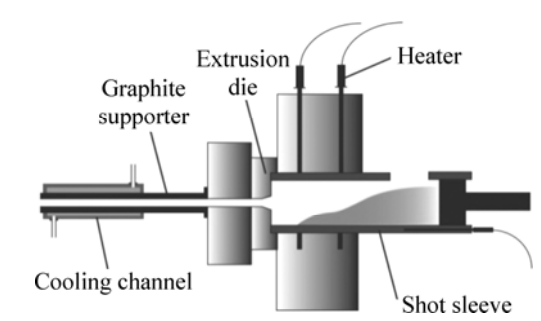


Fig.2 Schematic drawing of rheo-extrusion system

Table 2 Summary of parameters used in this study

Sample	Plunger	Solid	Temperature/°C		
code	speed/(cm·s ⁻¹)	fraction/%	Die	Sleeve	
SSM2-05	2	5	270	250	
SSM4-05	4	5	270	250	
SSM4-10	4	10	270	250	
SSM6-05	6	5	270	250	
SSM6-10	6	10	270	250	
SSM6-20	6	20	270	250	

2.2 Extrudability evaluation

The extruded samples were analyzed by the measurement of the length to determine the extrudability. The length of the samples was measured after the extrusion test. In this work, the criterion for the required length was 20 cm. Shorter samples were rejected.

2.3 Microstructure observation

The microstructure of the samples was observed using an optical microscope. The samples were cut and obtained from three positions as shown in Fig.3. The samples were then prepared for metallographic analysis using the standard grinding, polishing and etching procedure. Good extruded parts should have uniform microstructure throughout the length and along the radius.

2.4 Mechanical properties measurement

The samples that pass the criterion of extrudability

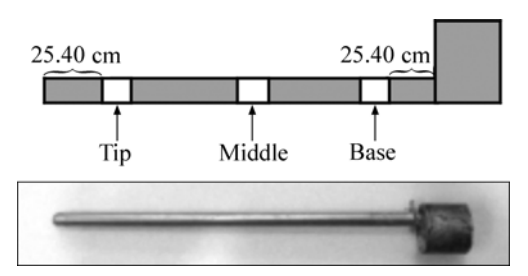


Fig.3 Sampling positions

were tested for the ultimate tensile strength and elongation using the universal testing machine (UTM). The sample was prepared using the ASTM B557M-02a standard[17].

3 Results and discussion

A representative extruded sample from the experiments is given in Fig.4. The results show that all the samples consist of unextruded, extruded and squeezed liquid sections. The samples produced by a lower plunger speed and at a higher solid fraction yield lower amount of squeezed liquid. These conditions tend to have less liquid segregation.

Observation of the surface shows that all the samples have a good surface finish in the extruded section as shown in Fig.5.

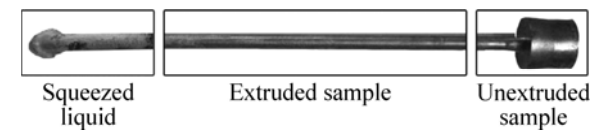


Fig.4 Components of representative rheo-extrusion sample

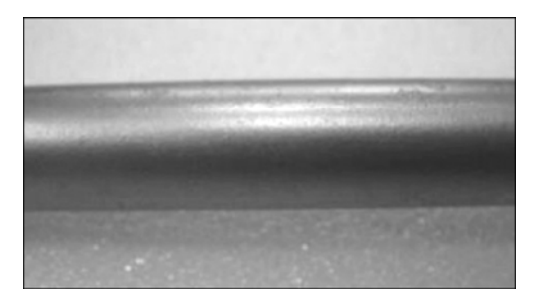


Fig.5 Surface finish of a representative sample

3.1 Extrudability

The samples produced by the conditions of 2, 4, and 6 cm/s plunger speed and 5% solid fraction have the lengths of 14, 23, and 24 cm, respectively. For 10% solid fraction, the samples produced by 4 and 6 cm/s plunger speed have the lengths of 18 and 23 cm, respectively. The sample produced by 20% solid fraction and 6 cm/s plunger speed has the length of 17 cm. The representative extruded samples from rheo-extrusion at different plunger speeds are shown in Fig.6.

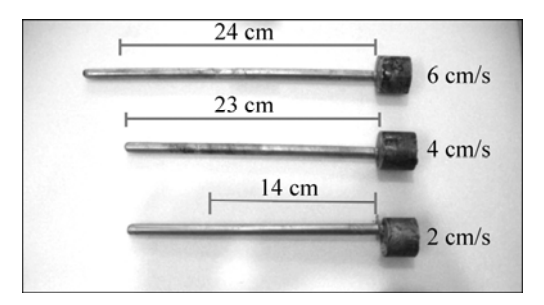


Fig.6 Samples from rheo-extrusion at different plunger speeds

The results suggest that conducting the rheoextrusion with a higher speed (6 cm/s) and with the lower solid fraction (5%) gives the longest length as expected since the slurry can flow easier and faster. In addition, at a higher solid fraction, the plunger speed needs to be higher to yield the same extruded length because of the increased viscosity of the slurry. When the solid fraction was too high (20%), the extruded sample was short since the solidification time was shorter and the viscosity was higher.

In summary, only the samples produced by the conditions of 5% solid fraction at 4 and 6 cm/s plunger speeds and 10% solid fraction at 6 cm/s plunger speed pass the requirement of the length, as shown in Table 3.

Table 3 Semi-solid extrudability of A356 Al-alloy

Plunger	Extrudability					
speed/(cm·s ⁻¹)	φ_s =5%	$\varphi_{s}=10\%$	$\varphi_{\rm s} = 20\%$			
2	×					
4	\checkmark	×				
6	\checkmark	\checkmark	×			

3.2 Microstructure uniformity

The microstructures at the center of the cross section of the three samples which pass the length criterion are shown in Fig.7. The micrographs show that the primary α structure (white structure) of all samples is quite similar and uniform in all the positions throughout the length. However, observation shows non-uniform microstructures in the radius direction in these samples. The edge of the samples (Fig.8) shows fine dendritic structure whereas the center of the samples shows semi-solid structure. The schematic drawing in Fig.8 illustrates the different structures at the edge and the center. The samples produced by the solid fractions of 5% and 10% have the length of liquid segregation zone of about 1.14 and 0.57 mm, respectively, as shown in Fig.9. It can be concluded that if the solid fraction increases, the liquid segregation around the outer perimeter will decrease.

The main result of using the starting slurry with low

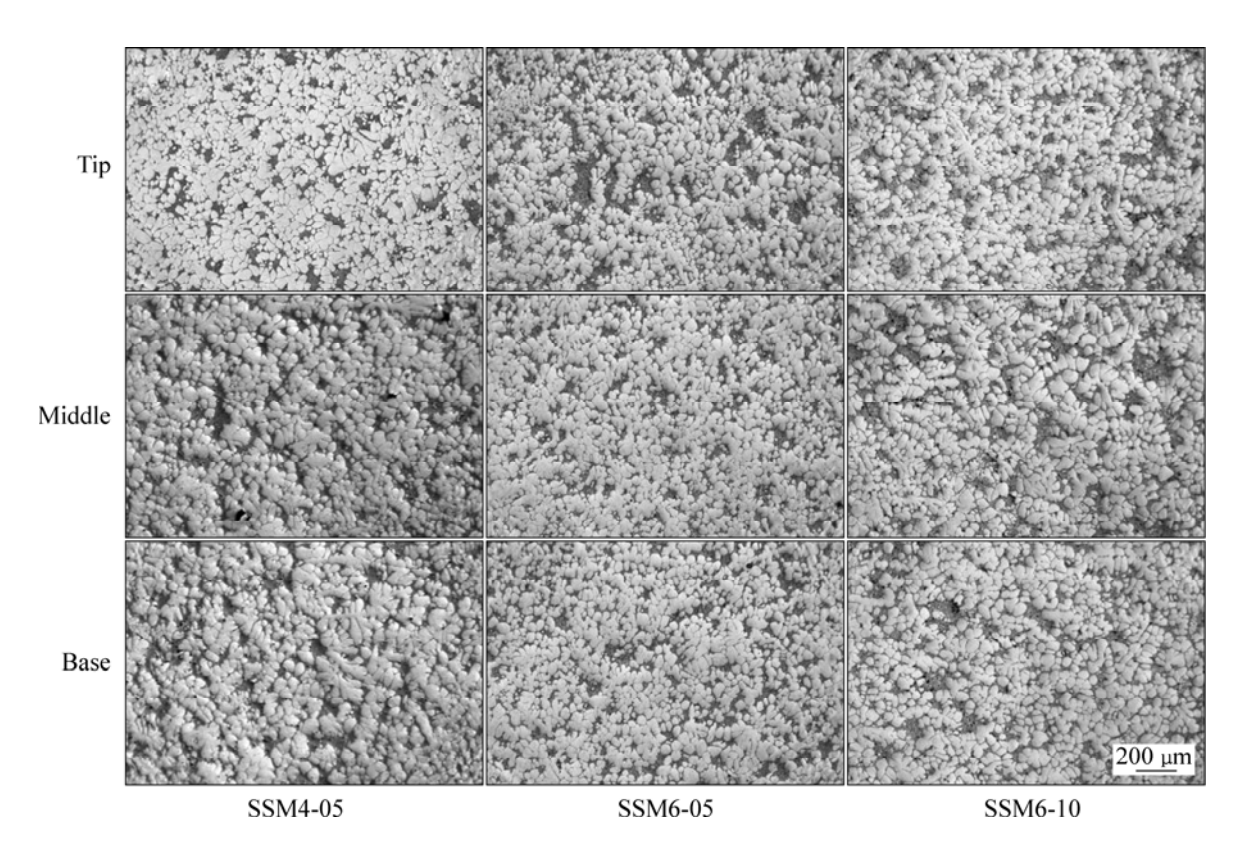


Fig.7 Representative microstructures of samples passing requirement of extrudability

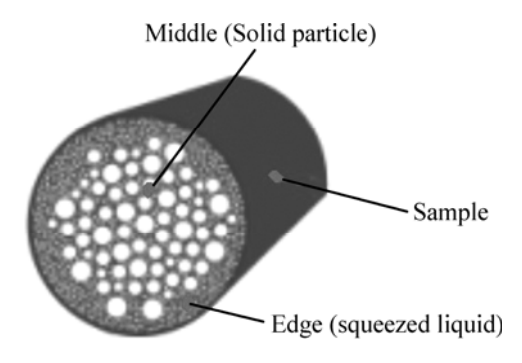


Fig.8 Schematic drawing showing liquid segregation in radius direction

solid fractions is the lubricating liquid segregation zone near the surface of the samples. The amount of the liquid segregation can be controlled by the amount of the starting solid fractions. Although the higher liquid segregation helps to lubricate the extrusion process, it should not be too much because it will lead to non-uniform microstructure which may affect the mechanical properties.

From the microstructure uniformity study, it can be concluded that the microstructures are uniform in the length direction for all the conditions of the plunger speeds and solid fractions of the slurry. In the radius direction, higher solid fraction results in the reduction of the liquid layer, which helps to increase the uniformity of the microstructure, as shown in Fig.9.

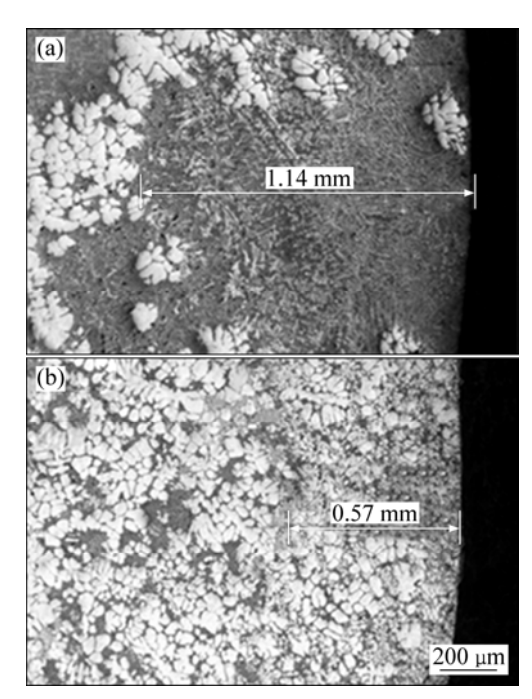
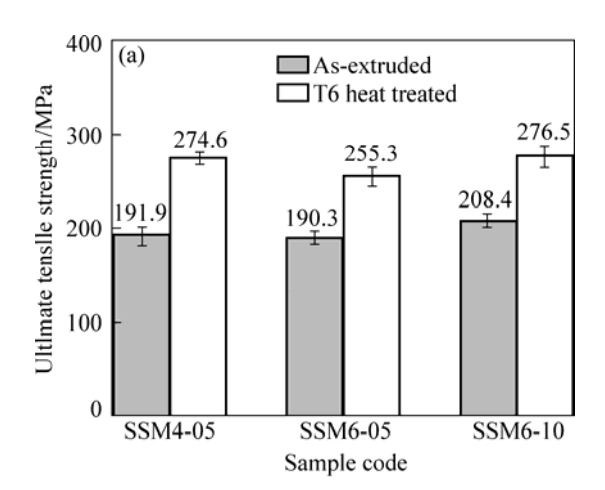


Fig.9 Representative microstructures at outer edge of samples at solid fractions of 5% (a) and 10% (b)

3.3 Mechanical Properties

The results of the mechanical property analysis report that the ultimate tensile strength and elongation of the as-extruded samples coded SSM4-05, SSM6-05 and SSM6-10 are 191.9 MPa, 190.3 MPa, 208.4 MPa and

7.5%, 6.5%, 11.2%, respectively. After T6 heat treatment, the ultimate tensile strength of samples is increased to 274.6 MPa, 255.3 MPa, 276.5 MPa and the elongation is increased to 8.3%, 7.3% and 12.4%, respectively. Fig.10 shows the ultimate tensile strength and elongation of the extruded samples before and after T6 heat treatment. The results show that the solid fraction and plunger speed do not significantly affect the tensile strength. In contrast, the results of the elongation indicate that the solid fraction affects the elongation. The elongation of the samples produced at 6 cm/s of plunger speed with 10% of solid fraction is higher than that of the samples produced at the same speed but at a lower solid fraction of 5%.



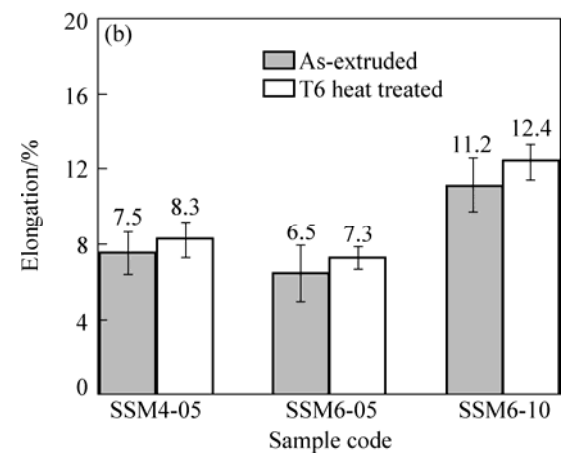


Fig.10 Ultimate tensile strength (a) and elongation (b) of extruded samples before and after T6 heat treatment

The higher elongation of the samples produced at a higher solid fraction may be the result of the lower liquid segregation in the radius direction as shown in Fig. 8 and Fig.9.

The comparison of the mechanical properties of the rheo-extruded 356 samples from this research and the typical extruded aluminum rod grade 6063 from ASM standard[16] is shown in Fig.11.

The results show that the rheo-extruded 356 samples have higher tensile strength than the 6063 alloy,

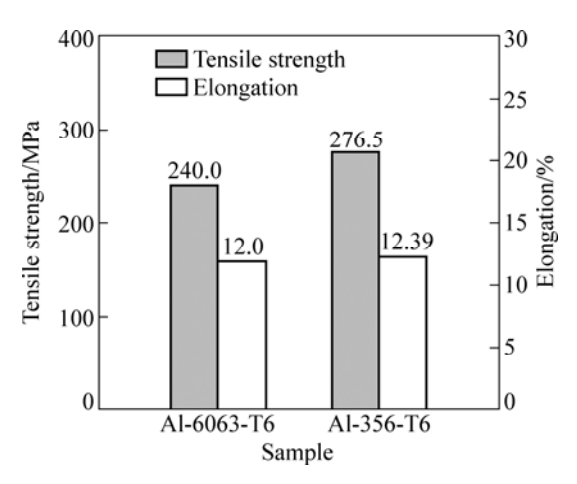


Fig.11 Comparison of mechanical properties of rheo-extruded 356 samples after T6 heat treatment from this research and typical extruded aluminum rod grade 6063 from ASM standard

and similar elongation property. Therefore, it can be concluded that the new rheo-extrusion process applying low solid fractions is a feasible process.

4 Conclusions

- 1) This preliminary study shows the feasibility of a new rheo-extrusion process using low starting solid fractions processed by the GISS technique. Good extruded products can be achieved with the appropriate conditions of solid fractions and plunger speeds.
- 2) In this rheo-extrusion using low solid fractions of the slurry, there is a liquid layer at the outer perimeter of the samples. This phenomenon helps to lubricate the flow of the extruded part. Therefore, the process can be used with higher plunger speeds in the semi-solid state compared with conventional hot extrusion.
- 3) Uniform microstructure in the length direction of the samples can be achieved in all conditions of the solid fractions and plunger speeds.
- 4) The ultimate tensile strength (UTS) does not depend on the solid fractions of the slurry and the plunger speeds. The samples from this rheo-extrusion of 356 aluminum alloy have higher strengths compared with commercial 6063 aluminum alloy.
- 5) The elongation of the samples depends on the solid fraction of the slurry. The higher solid fraction yields more uniform microstructure in the radius direction so that the elongation is improved.

Acknowledgements

The authors gratefully acknowledge the financial supports from Prince of Songkla University (Contract number AGR530031M) and the Thai Research Fund (Contract number MRG5280215). We also thank the Department of Mining and Materials Engineering,

Faculty of Engineering, Prince of Songkla University for the facilities and the Innovative Metal Technology (IMT) team for all the kind supports.

References

- PEARSON C, PARKINS R. The extrusion of metal [M]. London: Chapman & Hall Ltd, 1960: 223–270.
- [2] KALPAKJIAN S, SCHMID S R. Manufacturing processes for engineering materials [M]. New Jersey: Prentise Hall, 2008: 307–319.
- [3] FLEMINGS M C. Behavior of metal alloys in the semi-solid [J]. Metallurgical Transactions A, 1991, 22A: 957–981.
- [4] BAYOUMI M A, NEGM M I, EL-GOHRY A M. Microstructure and mechanical properties of extruded Al-Si alloy (A356) in the semi-solid state [J]. Materials and Design, 2009, 30: 4469–4477.
- [5] JANG D I, YOON Y O, KIM S K. Thixoextrusion for 7075 Al wrought alloy tube [J]. Solid State Phenomena, 2008, 141/142/143: 267–270.
- [6] MORADI M, NILI-AHMADABADI M, HEIDARIAN B, ASHOURI S. Investigation of thin wall casting made of semi-solid A356 using back extrusion and die cast [J]. Solid State Phenomena, 2008, 141/142/143: 67–72.
- [7] WANG K, ZHANG P, DU Y, ZENG P, LI H. Basic study on thixo-co-extrusion of multi-layer tube with Al/Mg alloys [J]. Solid State Phenomena, 2008, 141/142/143: 73–78.
- [8] SUGIYAMA S, LI J, YANAGIMOTO J. Semi-solid state extrusion of plain carbon steel [C]//The 8th International Conference on Semi-solid processing of Alloys and Composites. Limassol, Cyprus, 2004.

- [9] MIWA K, KAWAMURA S. Semi-solid extrusion forming process of stainless steel [C]//The 6th International Conference on Semi-solid processing of Alloys and Composites. Turin, Italy, 2000: 279–281.
- [10] KOPP R, KALLWEIT J, MOLLER T H. Thixoforming of steelexperiments with a vacuum chamber based tool concept [C]//The 6th International Conference on Semi-solid processing of Alloys and Composites. Turin, Italy, 2000: 599–604.
- [11] JORSTAD J L, THIEMAN M, KAMM R. Fundamental requirement for slurry generation in the sub liquidus casting process and the economics of SLCTM Processing [C]//The 8th International Conference on Semi-solid processing of Alloys and Composites. Limassol, Cyprus, 2004.
- [12] XU J, ZHANG S, YANG B, SHI S, FAN Z. Microstructure and mechanical properties of rheo-extruded AZ31Mg-alloy [J]. Solid State Phenomena, 2008, 141/142/143: 713-718.
- [13] JI S, FAN Z, BEVIS M J. Semi-solid processing of engineering alloys by a twin screw rheomoulding process [J]. Materials Science and Engineering A, 2001, 402: 170–176.
- [14] LEE B S, JOO D H, KIM M H. Extrusion behavior of Al-Cu alloys in the semi-solid state [J]. Materials Science and Engineering A, 2005, 402: 170–176.
- [15] WANNASIN J, JANUDOM S, RATTANOCHAIKUL R, FLEMINGS M C. Development of the gas induced semi-solid metal process for aluminum die casting application [J]. Solid State Phenomena, 2008, 141/142/143: 97–102.
- [16] HATCH J E. Aluminum properties and physical metallurgy [M]. Ohio: American Society for Metals(ASM), 1984: 363.
- [17] ASTM B557M-02a. Standard test methods of tension testing wrought and cast aluminum-and magnesium-alloy product[Metric] [M]. Pennsylvania: ASTM International, 2003: 1-15.

(Edited by YANG Bing)